Report No. UT-25.08

MOBILE-PHONE-BASED ARTIFICIAL INTELLIGENCE PACKAGE DEVELOPMENT AND VALIDATION IN LARGE SCALE FOR MAINTENANCE ASSET MANAGEMENT

Prepared For:

Utah Department of Transportation
Research & Innovation Division

Final Report
October 2024

RESEARCH
UDOT Keeping Utah Moving
Utah Department of Transportation - Research Division
4501 South 2700 West - P.O. Box 148410 - SLC,UT 84114-8410

DISCLAIMER

The authors alone are responsible for the preparation and accuracy of the information, data, analysis, discussions, recommendations, and conclusions presented herein. The contents do not necessarily reflect the views, opinions, endorsements, or policies of the Utah Department of Transportation or the U.S. Department of Transportation. The Utah Department of Transportation makes no representation or warranty of any kind, and assumes no liability therefore.

ACKNOWLEDGMENTS

The authors acknowledge the Utah Department of Transportation (UDOT) for funding this research, and the following individuals from UDOT on the Technical Advisory Committee for helping to guide the research:

- Shawn Lambert
- David Stevens
- Abdul Wakil
- Corey Unger
- Kevin Nichol
- Chris Whipple
- Benjamin Maughan
- Ryan Ferrin
- Brad Loveless

TECHNICAL REPORT ABSTRACT

1. Report No.	2. Government Accession No.	3. Recipient's Catalog No.
UT-25.08	N/A	N/A

4. Title and Subtitle	5. Report Date / 6. Performing Organization Code
Mobile-Phone-Based Artificial Intelligence Package Development and Validation in Large Scale for Maintenance Asset Management	5. Report Date: October 2024 6. Performing Organization Code: N/A
7. Author(s) Biao Kuang, Jianli Chen	8. Performing Organization Report No. N/A
9. Performing Organization Name and Address University of Utah Department of Civil & Environmental Engineering 110 Central Campus Drive, Suite 2000 Salt Lake City, UT 84112	10. Work Unit No. 5H092 16H 11. Contract or Grant No. 23-8957
12. Sponsoring Agency Name and Address Utah Department of Transportation 4501 South 2700 West P.O. Box 148410 Salt Lake City, UT 84114-8410	13. Type of Report & Period Covered Final Report May 2023 to October 2024 14. Sponsoring Agency Code PIC No. UT22.204

15. Supplementary Notes

Prepared in cooperation with the Utah Department of Transportation and the U.S. Department of Transportation, Federal Highway Administration

16. Abstract

Regular inspection of transportation assets is essential to maintain their optimal condition and functionality. Our previous UDOT-funded project (Contract No. 22-8099, Report No. UT-22.24) demonstrated significant promise of artificial intelligence in identifying various transportation assets through a mobile phone. However, the initial project was limited in scale, utilizing only ~1,000 images for training and validation. Therefore, this new project aims to extend our prior work. Specifically, this study increases the dataset to ~5,000 images for each targeted asset (i.e., pavement markings, litter & trash, traffic signs, and guardrails & barriers). Based on You Only Look Once (YOLO), a deep learning architecture, we trained four detection models capable of automatically identifying these objects with good accuracy metrics: F1 scores of 0.88 for pavement marking issues, 0.84 for litter/trash, 0.91 for traffic signs, and 0.96 for guardrails/barriers. Additionally, specific counting and geolocation models were developed to precisely quantify the number of identified objects within a road section or video clip and pinpoint the location of each detected object with the assistance of a phone-based GPS tracker. The geolocation model exhibits high performance in estimating object locations, with an average distance error of only 0.27 meters (about 0.9 feet). Furthermore, an interactive interface was created to visually represent the identified objects on a map, allowing for a comprehensive assessment of transportation asset conditions through intuitive visualizations. This new project enhanced our previous work by expanding the capabilities in detecting, counting, geolocating, and visualizing specific transportation assets, contributing to implementing regular transportation asset inspection and planning maintenance work, and thereby improving road safety.

17. Key Words	18. Distribution Statement	23. Registrant's Seal
Mobile phone, Artificial intelligence (AI), Transportation assets, Pavement marking, Traffic signs, Litter and trash, Guardrail and barrier	Not restricted. Available through: UDOT Research & Innovation Div. 4501 South 2700 West P.O. Box 148410 Salt Lake City, UT 84114-8410 www.udot.utah.gov/go/research	N/A

19. Security Classification (of this report)	20. Security Classification (of this page)	21. No. of Pages	22. Price
Unclassified	Unclassified	66	N/A

TABLE OF CONTENTS

LIST OF TABLES

LIST OF FIGURES

UNIT CONVERSION FACTORS

Generally, all measurements in the report are presented in inch-pound or US Customary system units. For non-conforming units, data conversion units are given in parentheses throughout the report. Partial conversion factors can be found in the table below.

SI* (MODERN METRIC) CONVERSION FACTORS				
APPROXIMATE CONVERSIONS TO SI UNITS				
Symbol	**When You Know**	**Multiply By**	**To Find**	**Symbol**
		LENGTH		
in	inches	25.4	millimeters	mm
ft	feet	0.305	meters	m
yd	yards	0.914	meters	m
mi	miles	1.61	kilometers	km
		AREA		
in^2	square inches	645.2	square millimeters	mm^2
ft^2	square feet	0.093	square meters	m^2
yd^2	square yard	0.836	square meters	m^2
ac	acres	0.405	hectares	ha
mi^2	square miles	2.59	square kilometers	km^2
		VOLUME		
fl oz	fluid ounces	29.57	milliliters	mL
gal	gallons	3.785	liters	L
ft^3	cubic feet	0.028	cubic meters	m^3
yd^3	cubic yards	0.765	cubic meters	m^3
		NOTE: volumes greater than 1000 L shall be shown in m^3		
		MASS		
oz	ounces	28.35	grams	g
lb	pounds	0.454	kilograms	kg
T	short tons (2000 lb)	0.907	megagrams (or "metric ton")	Mg (or "t")
		TEMPERATURE (exact degrees)		
°F	Fahrenheit	5 (F-32)/9 or (F-32)/1.8	Celsius	°C
		ILLUMINATION		
fc	foot-candles	10.76	lux	lx
fl	foot-Lamberts	3.426	candela/m^2	cd/m^2
		FORCE and PRESSURE or STRESS		
lbf	poundforce	4.45	newtons	N
lbf/in^2	poundforce per square inch	6.89	kilopascals	kPa
APPROXIMATE CONVERSIONS FROM SI UNITS				
Symbol	**When You Know**	**Multiply By**	**To Find**	**Symbol**
		LENGTH		
mm	millimeters	0.039	inches	in
m	meters	3.28	feet	ft
m	meters	1.09	yards	yd
km	kilometers	0.621	miles	mi
		AREA		
mm^2	square millimeters	0.0016	square inches	in^2
m^2	square meters	10.764	square feet	ft^2
m^2	square meters	1.195	square yards	yd^2
ha	hectares	2.47	acres	ac
km^2	square kilometers	0.386	square miles	mi^2
		VOLUME		
mL	milliliters	0.034	fluid ounces	fl oz
L	liters	0.264	gallons	gal
m^3	cubic meters	35.314	cubic feet	ft^3
m^3	cubic meters	1.307	cubic yards	yd^3
		MASS		
g	grams	0.035	ounces	oz
kg	kilograms	2.202	pounds	lb
Mg (or "t")	megagrams (or "metric ton")	1.103	short tons (2000 lb)	T
		TEMPERATURE (exact degrees)		
°C	Celsius	1.8C+32	Fahrenheit	°F
		ILLUMINATION		
lx	lux	0.0929	foot-candles	fc
cd/m^2	candela/m^2	0.2919	foot-Lamberts	fl
		FORCE and PRESSURE or STRESS		
N	newtons	0.225	poundforce	lbf
kPa	kilopascals	0.145	poundforce per square inch	lbf/in^2

*SI is the symbol for the International System of Units. (Adapted from FHWA report template, Revised March 2003)

LIST OF ACRONYMS

AI	Artificial Intelligence
ASTM	American Society for Testing and Materials
CNN	Convolutional Neural Network
DOT	Department of Transportation
EfficientDet	Efficient and Effective Detector
FN	False Negative
GPS	Global Positioning System
IoU	Intersection over Union
LiDAR	Light Detection and Ranging
mAP@50	mean Average Precision at 50
R-CNN	Region-Based Convolutional Neural Network
ResNet	Residual Network
SDD	Single Shot MultiBox Detector
TP	True Positive
UDOT	Utah Department of Transportation
YOLO	You Only Look Once

EXECUTIVE SUMMARY

Periodic inspection of transportation assets, such as pavement markings, traffic signs, and guardrails, is essential for preserving their optimal condition and functionality. Nevertheless, traditional inspection methods, often labor-intensive and reliant on manual assessment, suffer from inefficiencies and inaccuracies. The emergence of artificial intelligence (AI) technologies, e.g., deep learning and computer vision, is reshaping the inspection process through advanced data analysis and automation. In our previous UDOT Project (Contract No. 22-8099, Report No. UT-22.24), we developed an AI package for detecting transportation assets and related issues. However, the scope of our prior project was limited, employing only ~1,000 images for training and validation per task, lacking in generality and scalability. Therefore, this new project aims to expand upon our previous work and enhance our initially developed models.

First in the new project, we expanded the dataset to ~5,000 self-collected images for each targeted transportation asset, consisting of pavement marking issues, litter & trash, traffic signs, and guardrails & barriers. Based on the You Only Look Once (YOLO), a state-of-the-art deep learning architecture, we trained four AI detection models to identify these transportation assets automatically. The results reveal that the improved models exhibited strong detection capabilities, achieving F1 scores of 0.88 for pavement markings, 0.84 for litter, 0.91 for traffic signs, and 0.96 for guardrails and barriers.

We further extended our AI models to quantify the number of identified objects within a road segment or video clip. Based on object tracking, we developed a specialized counting model, which has been successfully deployed on a case study of a highway route in Utah. Moreover, we enhanced the AI packages to geolocate each identified object. By integrating a phone-based GPS tracker (GPX tracker) and employing time-based interpolations, we developed a geolocation model to match the video frames with GPS recorders. This model was designed to estimate the latitude and longitude of the identified objects accurately and exhibited high accuracy in pinpointing object positions, with an average distance error of only 0.27 meters (about 0.9 feet), which was validated through a case study on a test highway route (I-15) in Utah.

Finally, we employed Folium, a Python package, to develop an interactive interface for visually representing detailed information about identified objects on a map. These details included geolocation coordinates (latitude and longitude), object class, inspection timestamps, and cropped images. This interface serves as a valuable tool for transportation authorities, facilitating a comprehensive evaluation of transportation asset conditions through intuitive visualizations.

This project expands upon our previous work to enhance the detection of transportation assets, improving capabilities in identifying pavement markings, litter & trash, traffic signs, and guardrails and barriers, while introducing additional functionalities, such as counting, geolocating, and visualizing these detected objects. These advancements facilitate more frequent inspections of transportation assets, contributing to the continual enhancement of road user safety.

1.0 INTRODUCTION

1.1 Problem Statement

The good condition and functionality of transportation infrastructure are fundamental to functioning transportation networks, influencing daily life, public health, economic development, and social equity (Arezoumand & Smadi, 2024; Dowd et al., 2020). Pavement, pavement markings, traffic signs, and guardrails are the essential components of transportation networks, enabling the safe and efficient movement of people and goods (Akofio-Sowah et al., 2014; Chang & Vavrova, 2016; Kuhn et al., 2011). Given their critical importance, maintaining the safety and reliability of these infrastructure elements is needed for safeguarding public welfare and reducing potential hazards. Therefore, periodic inspection of transportation assets is fundamentally crucial to identify structural or appearance issues, such as wear, tear, and damage, and to ensure the integrity and functionality of these critical transportation assets (Karballaeezadeh et al., 2020; Sinha et al., 2017). Also, by conducting thorough inspections regularly, transportation authorities (e.g., State Departments of Transportation [DOTs]) are able to proactively address maintenance needs, fix issues, and prevent accidents or disruptions, ultimately enhancing safety and reliability. However, traditional inspection approaches, which are often labor-intensive and reliant on manual assessments, have limitations in terms of efficiency and accuracy (Le et al., 2024; Sinha et al., 2017). Human inspectors may inadvertently overlook subtle signs of deterioration and fail to detect potential issues that could compromise the integrity of infrastructure elements. Additionally, manual inspections are time consuming and resource intensive, causing delays in identifying and addressing maintenance needs in a timely manner (Farhadmanesh et al., 2021; Kuang et al., 2022).

By integrating artificial intelligence (AI) technologies such as deep learning and computer vision, transportation authorities are revolutionizing the inspection process through advanced data analytics and automation. AI algorithms are capable of analyzing vast amounts of data, including images, with remarkable speed and precision, which allows for the rapid and efficient detection of issues in transportation assets, automating and enhancing the accuracy of inspections. One application is pavement condition assessment (Farhadmanesh et al., 2021; Peng et al., 2024; Wen et al., 2022; Zakeri et al., 2017). Cano-Ortiz et al. (2022) pointed out that image-processing techniques perform well in detecting pavement distress, even using low-cost image-acquisition devices. Radopoulou & Brilakis (2015) developed a model for detecting road patches from video data collected by a camera mounted on a car, with high precision and recall rates. Noteworthily, the AI application has also been extended to other fields, for instance, pavement marking condition assessment and traffic sign identification (Karsten et al., 2021; Pike et al., 2010; Y. Zhang & Ge, 2012). Campbell et al. (2019) developed a model to detect and classify Stop and Give Way for monitoring the conditions of transportation assets based on Google Street View. Xu et al. (2021) assessed the pavement marking condition, i.e., determining the worn percentage, based on image segmentation and feature detection. However, generally, there is limited research applying the AI models to facilitate detecting or identifying pavement marking, litter on the roadside, guardrails and barriers, and traffic signs.

Our previously funded UDOT Project (Contract No. 22-8099, Report No. UT-22.24), titled *"Mobile Phone-Based Artificial Intelligence Development for Maintenance Asset Management,"* successfully developed an AI package capable of detecting certain transportation assets and issues, such as faded pavement markings, litter, traffic signs, and guardrails/barriers (Kuang et al., 2022). However, this study is small scale, with only ~1,000 images for model training and validation of each task. Additionally, the prior work is limited to identifying objects of interest but lacks the ability to count the number of detected objects within a specific road section or video clip. Object detection in the previous work is a static task focused on locating regions of interest in individual frames (Koch et al., 2013; Wang et al., 2023). However, the same object can appear across consecutive frames in a video sequence (Wei et al., 2021), leading to repeated detection of the same object in multiple frames.

Furthermore, the precise geolocation of identified objects is another gap in our previous project. Accurate geolocation is essential for planning effective maintenance work. A few prior studies have employed high-resolution Global Positioning System (GPS) devices to record geolocations during data collection (Ma et al., 2022; Okpe & Idachaba, 2023). Based on these GPS records, the location of detected objects can be inferred. However, the sampling rates of GPS devices and video recordings are heterogeneous, and how to accurately synchronize GPS records with video frames remains an unsolved issue in existing studies. This lack of precise location information for identified objects (e.g., transportation assets or asset issues) presents a significant research gap, which hinders maintenance teams from effectively understanding the locations of these issues for timely intervention.

1.2 Research Objectives and Tasks

To fill these research gaps, this project expands upon our previous work to conduct a large-scale study. Additionally, we aim to enhance our previous project by incorporating the ability to count and geolocate identified objects. To achieve these objectives, we propose the following research tasks:

Task 1: Data Collection: Increase the dataset size by collecting more images and videos of transportation assets and issues (pavement markings, traffic signs, trash, and guardrails) across a wider geographical area and different scenarios, e.g., low/strong illuminance days.

Task 2: Advance Object Detection Models: Incorporate more training data into the algorithm to develop and refine AI models for improving the performance of object detection in practice, i.e., the reliability and accuracy of object detection and condition assessment.

Task 3: Develop Model for Counting Objects: Develop algorithms, based on the detection models, to accurately count identified objects within a specific road section or video clip, reducing repeated detection in detections across consecutive video frames.

Task 4: Develop Model for Geolocating Objects: Synchronize GPS records with video frames to accurately geolocate the identified transportation assets and issues for reference of the maintenance team, filling the gap of missing geolocation of detected issues.

Task 5: Model Validation and Testing on a Large Scale: Conduct large-scale validation and testing of the improved AI models on the expanded dataset to ensure accuracy, reliability, and scalability.

1.3 Outline of Report

The remaining report is structured as follows: Section 2 reviews the pros and cons of current common practices in transportation asset data collection and applications of AI algorithms in various transportation asset maintenance. Section 3 introduces the methods used in this project and accuracy metrics to measure the performance of developed models. The results and performance of object detection, counting, geolocation, and visualization are presented in Section 4. Finally, Section 5 summarizes the key findings and recommendations for future work.

2.0 LITERATURE REVIEW

2.1 AI Applications in Identifying Transportation Assets

Various AI algorithms have been applied to transportation asset maintenance, with pavement condition assessment being a prominent research area. Commonly used deep learning methods include CNN (Gopalakrishnan et al., 2017), Faster R-CNN (Majidifard et al., 2020), and YOLO (Mandal et al., 2020). Numerous public datasets related to pavement distress have been collected via smartphones, cameras, and Google Street View images (Majidifard et al., 2020; Mandal et al., 2020). Using these AI models and data sources, multiple types of pavement distress, (e.g., transverse cracks, longitudinal cracks, block cracks, potholes, and alligator cracks) can be automatically identified with high accuracy (Du et al., 2020; Ghosh & Smadi, 2021; Majidifard et al., 2020). Additionally, several studies have focused on pavement issues specific to certain pavement types, such as asphalt (K. C. P. Wang et al., 2017; Wen et al., 2022) and Portland cement concrete (Gopalakrishnan et al., 2017). Some exceptional cases have also been explored, such as object detection in non-ideal photographic conditions, including low illumination or shadows cast by nearby objects (Tepljakov et al., 2019).

2.1.1 Pavement Marking Detection

Relatively few studies have been conducted to assess pavement marking conditions, among which one commonly employed approach is to quantify the ratio of remaining pavement markings directly. Lee & Cho (2023) utilized Mask R-CNN to develop a model for the automatic calculation of pavement-marking defect ratios through the retroreflectivity of markings collected by a vehicle-mounted retroreflectometer. Visual images are also usually adopted. Zhang & Ge (2012) adopted some traditional image processing methods (e.g., Hough transformation and feature recognition) to determine the percentage of remaining pavement markings automatically. Xu et al. (2021) quantified the faded severity level of pavement markings by measuring the worn percentages at the pixel level based on image processing techniques, such as edge extraction and object segmentation. Likewise, the work of Kang et al. (2020), based on YOLOv3, has the capability to identify the arrow markings and evaluate the visibility of markings by computing intensity contrast between pavement markings and the surrounding markings. Wei et al. (2021) estimated the damage ratio of pavement markings by segmenting the regions of the original marking and faded marking based on hierarchical semantic segmentation methods.

Another vision-based method to assess pavement marking conditions is identifying pavement marking issues through deep learning and computer vision techniques. Iparraguirre et al. (2022) utilized multiple deep learning architectures, including Faster R-CNN, SDD, and EfficientDet, to identify faded markings. However, they only considered one class (white faded lane marking) and did not provide a clear description of the data labeling criteria. Alzraiee et al. (2021) classified faded markings into nine classes and utilized faster R-CNN to train a model to detect marking issues automatically. However, the accuracy is relatively low, with an accuracy of less than 0.25. Kawano et al. (2017) and Bronuela-Ambrocio & Antes (2023) applied YOLO to detect the faded conditions of marking; however, the accuracy scores of the two studies are also not decent (precision < 60%). Sun et al. (2024) compared the performance of YOLOv5, YOLOv7, Faster R-CNN, and ResNet in detecting pavement marking defects using 2,000 self-labeled images, with an accuracy ranging from 0.86 to 0.94. The CNN-based model developed by Maeda et al. (2018) is able to identify two types of pavement marking issues: faded cross walk and white faded line marking, with the accuracy ranging from 0.62 to 0.95. Kong et al. (2022) adopted the DeepLab V3+ semantic segmentation model to assess the defects of line markings, arrow markings, and evenly spaced line markings with F1 values from 0.81 to 0.85. However, it is worth noting that the above-related studies only consider some particular shapes of pavement markings (e.g., lane markings) while neglecting the faded issues of other pavement markings.

2.1.2 Traffic Sign Detection

Another common application of AI algorithms in transportation asset management is the identification of traffic signs. In the past, traditional feature-based image processing techniques were commonly used for automatic traffic sign detection. For example, Kim et al. (2012) developed a model to detect speed signs based on color and shape features, achieving a detection rate of 93%. Similarly, Balali & Golparvar-Fard (2014) proposed a model to classify traffic signs using color and shape, with an accuracy of 79.3% in classifying different traffic signs.

With the development of deep learning and computer vision, traditional feature-based methods for traffic sign detection have been largely replaced by neural networks that can directly classify or detect traffic signs (Nguyen et al., 2023). Instead of relying on predefined features like color and shape, deep learning models automatically learn relevant patterns from large datasets. These models, particularly convolutional neural networks (CNNs), have proven highly effective at accurately identifying and classifying traffic signs in real-time, significantly improving performance over earlier methods. Hoang et al. (2018) combined various computer vision techniques, such as image augmentation and region processing, with CNNs to develop an AI model for traffic sign recognition. Similarly, Tabernik & Skočaj (2020) utilized the Mask R-CNN deep learning model to create an automatic traffic-sign inventory management system, encompassing 200 categories of traffic signs. Using an open-source dataset from Google Street View images, Campbell et al. (2019) built a training dataset and developed a deep learning model to identify Stop and Give Way signs. Kargah-Ostadi et al. (2020) employed MobileNetV2 SSDLite to recognize approximately 40 types of traffic signs, achieving an average accuracy of 0.89. Additionally, the robustness of automatic traffic sign detection under challenging conditions such as snowy days and low illumination has been explored (Chehri et al., 2021; Khan et al., 2018).

2.1.3 Litter and Trash Detection

Compared to pavement issues, fewer studies have focused on litter and trash recognition on roads (Wu et al., 2023). Wu et al. (2023) reviewed existing research on automatic litter detection and found that only 10.4% of the studies focused on urban trash. Rad et al. (2017) developed a model to identify litter, such as cigarettes and leaves, and quantify their presence. Liu et al. (2018) applied YOLOv2 to detect garbage on pavements but only considered a single class of trash. Similarly, the AI model developed by Sayyad et al. (2020) did not classify different types of garbage and was limited to detecting large-sized trash. Zhang et al. (2019) used Faster R-CNN to automatically identify and count different categories of litter, including organic, inorganic, trash, and tree leaves. However, the dataset was entirely collected from street roads, limiting its applicability to highway environments. Mandhati et al. (2024) compared the performance of Faster R-CNN, RetinaNet, YOLOv3, and YOLOv5 for detecting plastic litter on roadsides, achieving an average precision of 40%. V et al. (2022) developed a YOLOv4-based model to detect plastic bottles and trash cans using 343 images, with a precision of 0.71 and recall of 0.81.

2.1.4 Guardrail and Barrier Detection

Furthermore, research on detecting steel guardrails and concrete barriers is relatively limited. Hou et al. (2022) and Hou & Ai (2022) developed network models for detecting W-beam guardrails and concrete barriers, respectively, using 3D local feature extraction from mobile LiDAR data. In contrast, for RGB images, Z. Liu et al. (2020) created a standard urban image database with eight categories of urban images, including damaged traffic guardrails. Jin et al. (2021) combined feature extraction with Mask R-CNN to detect steel guardrails on highways, although their model did not address concrete barriers.

2.1.5 Brief Summary

Overall, deep learning and computer vision models have demonstrated outstanding performance in automatic object detection and image classification. These techniques have been widely applied across various fields, including transportation asset monitoring and inspection. Pavement condition assessment is one of the most extensively researched areas, followed by traffic sign identification, showcasing the great potential of using AI for automatic, efficient, and affordable transportation asset identification and assessment. However, relatively less research has focused on identifying pavement marking issues, with some types of markings often overlooked. Additionally, there is a notable lack of studies on identifying steel guardrails, concrete barriers, and litter or trash on roads.

2.2 AI Applications in Object Counting

Quantifying the quantity of identified objects, e.g., the issues of transportation assets, is crucial information for infrastructure inspection. For instance, determining the number of faded markings within a specific road segment is essential for assessing the degree of deterioration in pavement markings and determining the necessity for repainting. In video detection, however, consecutive frames may record the same object, and there is a lack of studies to count these objects for this purpose. Although Okpe & Idachaba (2023) claimed their works are able to count the pavement potholes, the counting is still the number of detections, which does not consider duplicate detections of the same objects in different video frames. Therefore, in practical applications, the actual number would be less than the number counted by their developed model. Wei et al. (2021) noticed the duplicate detections of the same object in multiple frames of video and utilized Kernelized Correlation Filters to track markings in video frame sequences. However, they did not make tracking to count the actual number of faded markings in a road section. Noteworthily, object tracking can distinguish the same object in different video frames, which provides a potential solution to count the actual number of faded markings.

Multi-object tracking and counting algorithms have been widely used in transportation areas, for example, vehicle and pedestrian counting (Fernández-Sanjurjo et al., 2019; Wickramasinghe & Ganegoda, 2020), but is less applied to count the detected infrastructure assets, e.g., pavement marking issues. A few studies employed tracking and counting models to count the other transportation assets. Koch et al. (2013) adopted a kernel-based tracking method to count the number of potholes within a sequence of video frames. Ma et al. (2022) utilized YOLOv3 to detect pavement cracks, followed by the Median Flow to track the detected cracks and count the number of cracks in the road section.

2.3 AI Applications in Geolocating Objects

Geolocation of identified issues is another critical piece of information for planning the maintenance work of transportation assets; however, it is often absent in the majority of studies related to detecting and assessing transportation assets. Some studies have used geo-labeled images. For instance, Kong et al. (2022) assessed pavement marking conditions using street-view imagery from open-source maps, which included GIS data and images. Similarly, Kargah-Ostadi et al. (2020) integrated GPS information with their data, allowing for precise geolocation of transportation assets in each image. While effective, this method is not ideal for self-collected data or frequent updates, as it relies on existing street-view inventories.

Other studies have employed specific GPS devices to collect geolocation data with videos/images to identify issues of transportation infrastructures (e.g., pavement). Okpe & Idachaba (2023) integrated a GPS module with a Raspberry Pi to record pothole locations and simultaneously transmit the data to monitoring systems via email. Similarly, Ma et al. (2022) developed a custom detection device featuring a 4G wireless module and GPS to pinpoint pavement cracks. In both cases, specialized GPS devices were necessary. Mobile phones have also been utilized in similar studies to collect images and GPS data simultaneously. For instance, Souza et al. (2018) used a mobile phone app to collect GPS data at a rate of 1 Hz to assess pavement conditions along a road section. However, their study required only low-resolution geolocation data, focusing on the road section as a whole rather than pinpointing the specific location of each pavement issue.

3.0 METHODOLOGY

3.1 Research Process Overview

The AI package development workflow is illustrated in Figure 3.1.

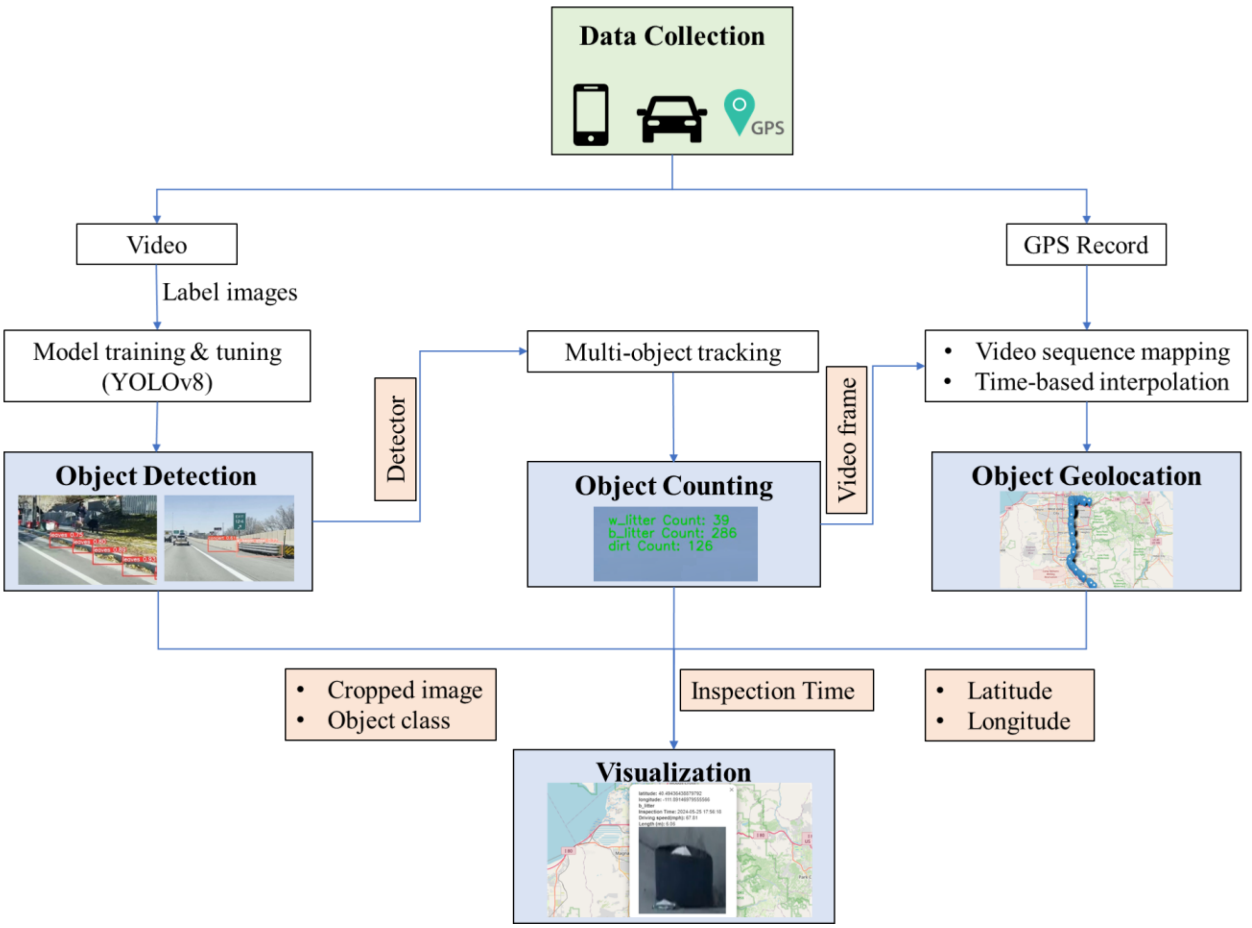

Figure 3.1 Research Framework

First, a mobile phone is mounted on the front windshield of vehicles to collect data, including video and GPS driving information. These videos are then transformed into images and annotated for training and validation of detection models, utilizing the You Only Look Once (YOLO), for various targeted transportation assets, including pavement markings, litter and trash, traffic signs, and guardrails and barriers. Subsequently, based on the developed detector and multi-object tracking methods, a counting model is created to quantify the number of identified objects within a road section or video clip. During the counting development, the video frames of each identified object are obtained, based on which we further develop a geolocation model to map GPS records with video frames. Through time-based interpolations, another model is formulated to estimate the geolocations of each identified object (i.e., latitude and longitude). Ultimately, by integrating the outputs of the aforementioned models, a visualization interface is developed to display the details of detected objects on an interactive map. This interface includes cropped images, object classifications, geolocations, and inspection timestamps.

3.2 Data Collection and Processing

Consistent with Phase I, this project uses a mobile phone, mounted on the front windshield of a vehicle on the passenger side to collect the data of transportation assets from a front view. The setup of data collection is shown in

Figure **3.2**. The collected videos are in 30 frames per second (fps) and are collected on both freeways and local streets in Utah, which cover varying scenarios, including different road sections and illuminance levels. These videos collect all types of transportation assets targeted in the project, including pavement markings, traffic signs, steel guardrails and concrete barriers, and litter & trash.

(a) Exterior View (b) Interior View

Figure 3.2 Setup of Data Collection

During data processing, each image frame from the recorded videos is sequentially extracted. To build the dataset, only the frames that clearly capture the objects of interest are manually selected. To minimize redundancy, at most three frame images recording the same object are chosen for training purposes, ensuring diversity while avoiding the overrepresentation of any single object.

3.3 Data Annotations

We use LabelImg[1] to label objects with bounding boxes for the development of our training and test datasets. LabelImg is a free and open-source graphical annotation tool that enables us to label objects for this project accurately. Our dataset is labeled separately for different tasks, each corresponding to specific targeted transportation assets, to either identify them or assess their conditions.

In this project, we categorize pavement markings into white and yellow classes and assess their conditions accordingly. Following guidelines from ASTM (2020), markings with over 50% of their areas faded or missing were labeled as "faded," excluding fully faded markings. Faded markings are further classified into two classes: "y_faded" (yellow faded markings) and "w_faded" (white faded markings). The "y_faded" category includes faded yellow curb or lane markings, both single and double, while the "w_faded" category encompasses faded white longitudinal lane markings, horizontal markings (e.g., crosswalks, stop lines), arrow markings, and word markings.

Additionally, this project classifies trash and litter on pavement into four types: (1) "leaves," including vegetation and leaves along the roadside; (2) "dirt," referring to dirt on the roadside; (3) "w_litter," consisting of litter in white or light colors (e.g., plastic and foam); and (4) "b_litter," representing litter in black or dark colors (e.g., used tires, rubber, and branches).

---

[1] https://github.com/heartexlabs/labelImg

For traffic signs, we follow the classification outlined in the *Manual on Uniform Traffic Control Devices* (FHWA, 2009), dividing them into four types: (1) **Regulatory signs**: stop signs, yield signs, and "Do not enter" signs (mostly in red or white); (2) **Speed signs**: speed limit and school zone signs (mostly in white); (3) **Warning signs**: warning signs and object markers (mostly in yellow); (4) **Guide signs**: destination guide signs and traffic movement signs (mostly in green).

Lastly, this project also categorizes guardrails and barriers into two classes: (1) **Concrete**: including cast-in-place concrete barriers and New Jersey-shaped barriers; (2) **Steel beam**: comprising w-beam guardrails and w-beams with steel blocks.

3.4 Model Development for Object Detection

You Only Look Once (YOLO) is an object detection model with high accuracy and speed due to simultaneous detection and classification (Redmon et al., 2016). In this study, we selected YOLOv8 as the deep learning architecture to train detection models for identifying various targeted transportation assets, including pavement markings, litter and trash, traffic signs, and guardrails and barriers. In the detection process, YOLO predicts bounding boxes and associated class probabilities directly from full images. Only results with a probability larger than or equal to the probability threshold (0.35 in this study) will be output. Also, YOLO can crop the detected objects for further processing.

In this study, we adopted three metrics to evaluate the performance of the trained mode, as defined in equations (1)-(3). Specifically, a prediction box will be considered as a correct detection, i.e., true positive (TP), if its Intersection over Union (IoU) with the ground truth box exceeds a predefined threshold (0.65, used in our experiments). Otherwise, it is considered as a false positive (FP), including any background object captured by a prediction box. False negative (FN) means the faded markings in white or yellow have not been detected by any prediction box. Precision reflects the reliability in classifying objects as positive, while recall measures the ability of the model to detect positive objects (i.e., TP). To avoid outperforming in one of the two metrics (precision and recall) but underperforming in the other, the F1-score is introduced to balance recall and precision by weighting them equally. Furthermore, to provide a more comprehensive assessment of the detection mode performance, we introduced an additional dimension - Mean Average Precision at 50% (mAP @50). mAP@50 signifies the mean average precision computed at an IoU threshold of 0.50. The higher the values of the three metrics, the better the results.

$$precision = \frac{TP}{TP+FP} \tag{1}$$

$$recall = \frac{TP}{TP+FN} \tag{2}$$

$$F1 = \frac{2*precision*recall}{precision+recall} \tag{3}$$

3.5 Model Development for Object Counting

The fundamental concept of object tracking, as illustrated in Figure 3.3, involves the continuous monitoring of identified objects across consecutive video frames by leveraging both spatial and temporal features (Wojke et al., 2017). This process ensures consistent tracking of each detected object by updating bounding box coordinates and assigning unique identifiers. Object tracking encompasses object detection and motion prediction through data association techniques.

In the architecture of YOLOv8, Byte Track stands out for its focus on tracking by detecting and maintaining object identities with decent precision across frames. Byte Track exhibits robustness in diverse settings, adeptly handling complex environments, variable lighting conditions, and occlusions. Hence, we select Byte Track as the foundational methodology for assigning IDs to detected objects and subsequently quantifying the number of objects within each video frame.

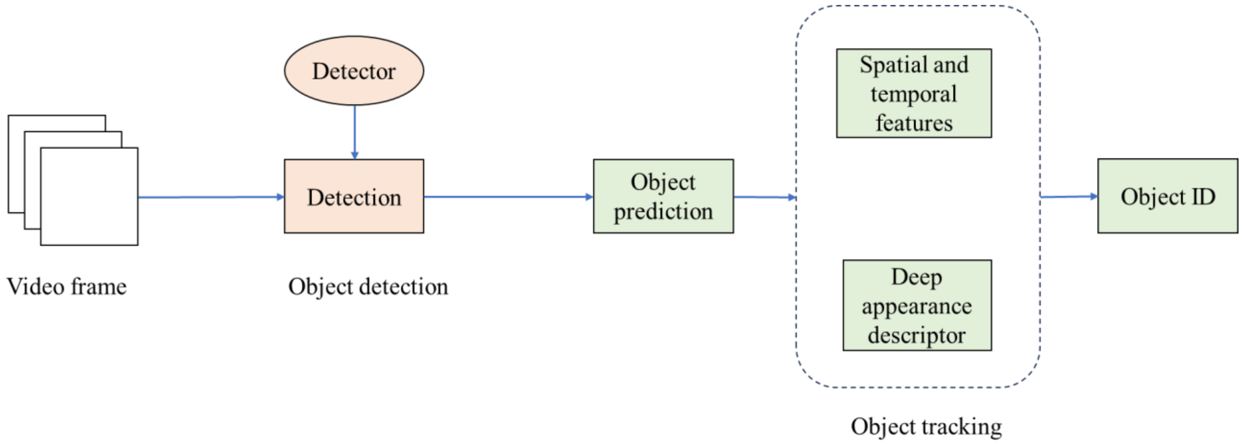

Figure 3.3 Illustration of Object Tracking

3.6 Model Development for Geolocating Object

During video collection, an open-source GPS tracker application, named GPX Tracker, is installed and utilized to capture the geolocations of the vehicle along with video collection for further locating the issues of pavement markings.

During the data collection, videos are shot at 30 frames per second, while the sampling rate of the GPX tracker varies by moving speed and is at most 2 times per second. GPX tracker records the latitude (*lat*), longitude (*lon*), elevation (*ele*), and the corresponding timestamp (*time_gpx*), indicating when the location data was recorded. The timestamp of the GPX tracker has a time accuracy of only up to seconds; as a result, the different locations may be recorded at the same timestamp. Additionally, the time accuracy of each video frame can reach milliseconds. Therefore, the faded markings captured by the video frame are unable to match GPX records precisely due to the different sample rates.

To solve this issue, we developed a model to locate the faded pavement markings. The main processes are as follows:

(1) The issues of pavement markings are detected by Model I, with the output of the class (*cls*) and cropping image (*img*) of the faded markings. The timestamp of identified marking issues (*time_img*) can be inferred based on the number of frames and video start recording time.

(2) Identified marking issues are matched with their nearest GPX records based on their timestamps (i.e., *time_img* and *time_gpx*, respectively).

(3) Due to the short distance within a few seconds, the location (latitude and longitude) of each identified marking issue is estimated based on the second closest records before and after the corresponding matched GPX record using linear interpolations based on the time differences, as illustrated in Figure 3.4 and equations (4) and (5). For example, $time_{img}$ =10:01:27.96 (accuracy up to milliseconds) matches with $time_{gpx}$ at $time_{idx}$ =10:01:27 (accuracy up to seconds). The second closest points before and after the $time_{idx}$ are $time_{idx-2}$ and $time_{idx+2}$, i.e., 10:01:26 (*time1*) and 10:01:28 (*time2*) in the example. Based on the time differences between $time_{img}$, $time_{idx+2}$, and $time_{idx-2}$, the location of the identified marking issue at $time_{img}$ (lat_{img} and lon_{img}) can be estimated.

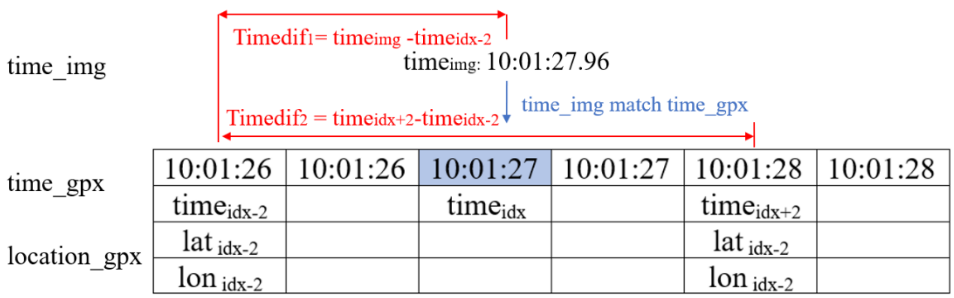

Figure 3.4 Illustration of Geolocation Estimation

$$lat_{img} = lat_{idx-2} + (lat_{idx+2} - lat_{idx-2}) * \frac{(time_{img} - time_{idx-2})}{time_{idx+2} - time_{idx-2}} \quad (4)$$

$$lon_{img} = lon_{idx-2} + (lon_{idx+2} - lon_{idx-2}) * \frac{(time_{img} - time_{idx-2})}{time_{idx+2} - time_{idx-2}} \quad (5)$$

Where $time_i$ is indicated in Figure 3.4, lon_i and lat_i are the longitude and latitude of the location at $time_i$.

4.0 RESULTS

4.1 Results of Object Detection

Our detection models were trained individually for each task using a desktop system equipped with an 8-Core CPU, an NVIDIA GeForce RTX 3070 GPU, and 64GB of memory. The training was conducted based on the YOLOv8 architecture to ensure optimal performance and accuracy for the tasks in this project.

4.1.1 Identifying Pavement Marking Issues

There are a total of 7,000 images labeled for pavement marking issues, which have been subdivided into training and validation sets, with 5,600 images for training and 1,400 images for validation, following an 8:2 ratio. The best model training result was achieved at epoch 173. Figure 4.1 illustrates the training loss and accuracy metrics during the algorithm training process, which finally reaches convergence. The model has a precision of 0.88, recall of 0.89, F1-score of 0.89, and mAP50 of 0.93 on average, as shown in Table 4.1. Also, the trained model has relatively higher performance in identifying yellow faded markings than white faded markings, with higher accuracy metrics.

Figure 4.2 shows various examples demonstrating the capabilities of the model in detecting white and yellow faded markings. The white faded markings include single-lane markings, word markings, and arrow markings, whereas the yellow faded markings consist of both double- and single-lane markings. The model performance has also been validated on tiger markings (i.e., contrast black striping used adjacent to white striping), demonstrating that the contrast striping does not affect the evaluation results for the white markings.

Table 4.1 Accuracy Metrics of Identifying Faded Pavement Markings

Class	Precision	Recall	F1-score	mAP50
all	0.88	0.89	0.88	0.93
w_faded	0.86	0.86	0.86	0.91
y_faded	0.91	0.91	0.91	0.95

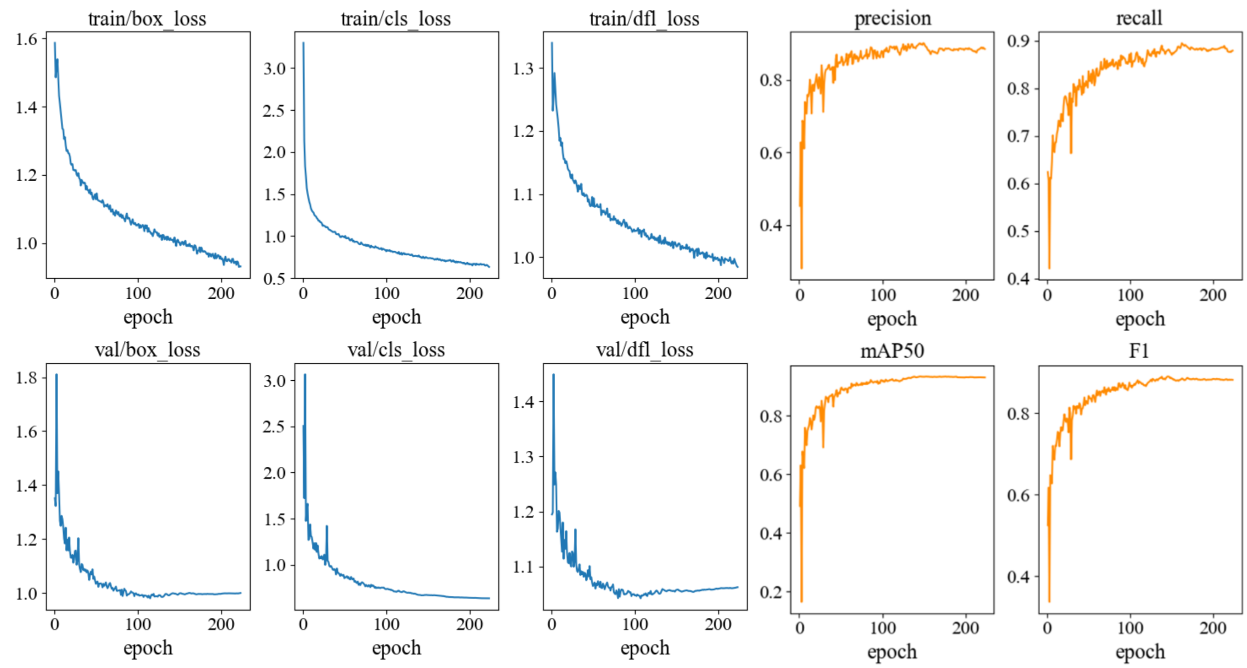

(a) Training Loss (b) Accuracy Metrics

Figure 4.1 Training Loss and Accuracy Metrics of Model for Pavement Marking Issue

Note: Epoch refers to one complete pass through the entire training dataset by the model.

(a) Faded White Lane Marking-1

(b) Faded White Lane Marking-2

(c) Faded White Word Marking-1

(d) Faded White Word Marking-2

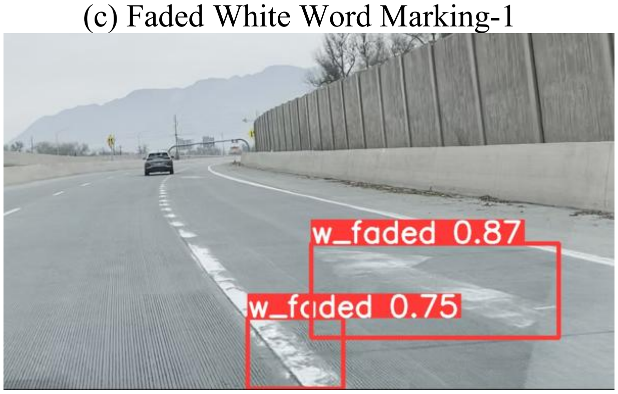

(e) Faded White Arrow and Lane Markings-1

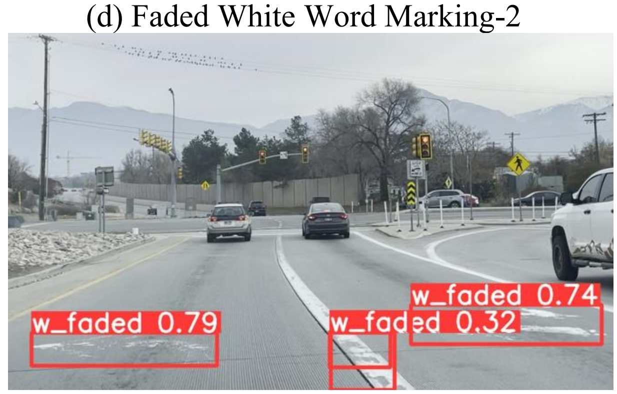

(f) Faded White Arrow and Lane Markings-2

(g) Faded Yellow Single Lane Marking

(h) Faded Yellow Double Lane Marking

Figure 4.2 Examples of Detection Results of Pavement Marking Issues

However, the developed model for pavement-marking issue detection has some limitations. It fails to differentiate between previously removed markings and faded markings; for instance, in Figure 4.3 (a), the model misclassifies the previously removed marking as a faded marking. Additionally, it is not able to identify some almost fully faded markings, as seen in Figure 4.3 (b). In other scenarios, the model may incorrectly detect other markings or objects with white elements (e.g., pieces of snow) as faded markings, as illustrated in Figure 4.3 (c)-(e).

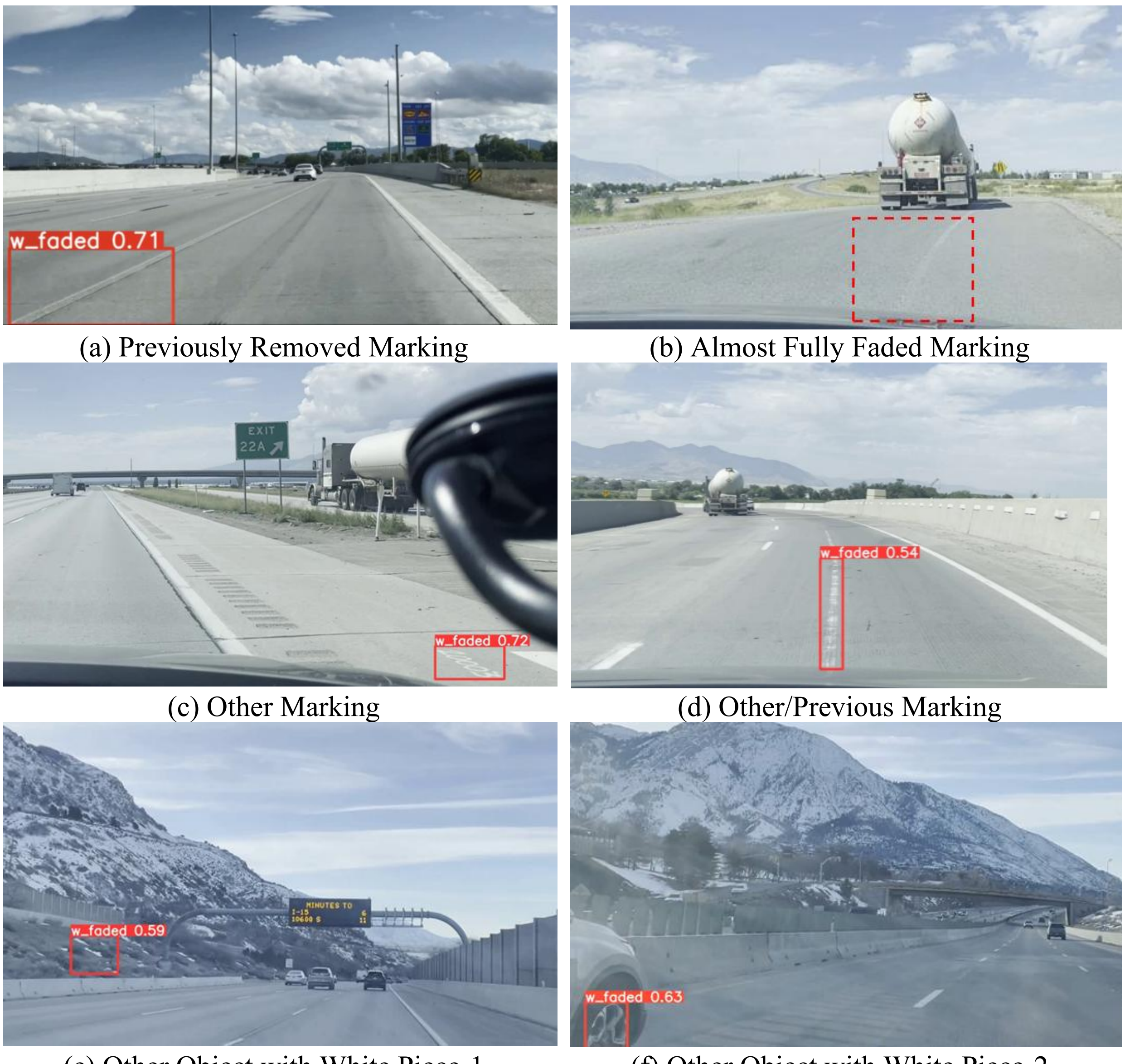

(a) Previously Removed Marking
(b) Almost Fully Faded Marking
(c) Other Marking
(d) Other/Previous Marking
(e) Other Object with White Piece-1
(f) Other Object with White Piece-2

Figure 4.3 Examples of Wrong Detection of Pavement Marking Issues

4.1.2 Identifying Litter & Trash

A total of 6,250 images covering litter and trash on the roadside have been labeled and partitioned into training and validation datasets, with 5,000 images designated for training and 1,250 images for validation. Then, a model was specifically trained to identify litter and trash on the roadside. Figure 4.4 shows the plots of the training loss and accuracy metrics tracked during the algorithm training phase for this model. The optimal training point was reached at epoch 219. The performance metrics of the model are as follows: precision of 0.86, recall of 0.82, F1-score of 0.84, and a mAP50 of 0.88, as detailed in Table 4.2.

In Figure 4.5, a selection of examples is presented showcasing the performance of the trained model in detecting trash and litter along the roadside. These examples include various types of debris, such as black litter (e.g., tire), white litter (e.g., plastics), leaves, and dirt.

Table 4.2 Accuracy Metrics of Trash & Litter

Class	Precision	Recall	F1 score	mAP@50
all	0.86	0.82	0.84	0.88
leaves	0.82	0.80	0.81	0.84
dirt	0.86	0.82	0.84	0.88
w_litter	0.87	0.82	0.84	0.90
b_litter	0.88	0.83	0.85	0.90

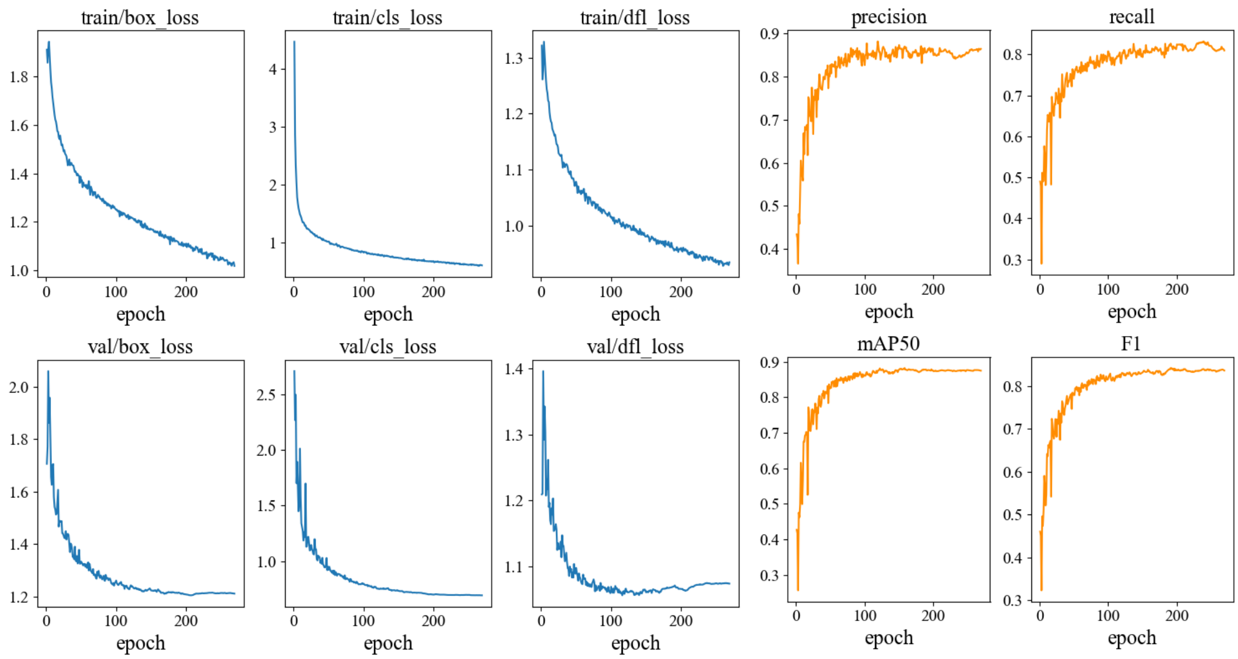

(a) Training Loss (b) Accuracy Metrics

Figure 4.4 Training loss and accuracy metrics of model for litter & trash

(a) Black Litter on the Highway-1
(b) Black Litter on the Highway-2
(c) White Litter on the Highway-1
(d) White Litter on the Highway-2
(e) Leaves on the Street Road-1
(f) Leaves on the Street Road-2
(g) Dirt on the Highway-1
(h) Dirt on the Highway-2

Figure 4.5 Examples of Detection Results of Trash & Litter

The model for litter identification also has certain limitations. It may mistakenly identify some pavement issues as litter; for instance, asphalt patches, black stains, or cracks on the pavement are classified as "b_litter," as illustrated in Figure 4.6 (a)-(d). Similarly, certain white marks or gray objects, such as stones, may be misclassified as "w_litter," as shown in Figure 4.6 (e) and (f).

(a) Previously Removed Marking

(b) Almost Fully Faded Marking

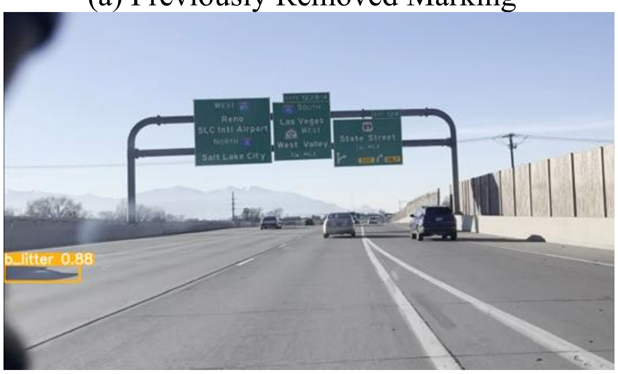

(c) Other Marking

(d) Other/Previous Marking

(e) Other Object with White Piece-1

(f) Other Object with White Piece-2

Figure 4.6 Examples of Wrong Detection of Trash & Litter

4.1.3 Identifying Traffic Signs

The dataset of traffic signs is 5100 images, including 4080 images for training and 1020 for validation. Figure 4.7 displays the training loss and accuracy metrics of the model designed to identify traffic signs. The optimal performance of the model is achieved at epoch 241. It exhibits strong performance in recognizing various types of traffic signs, including regulatory, speed limit, warning, and guide signs, with decent metrics: an average precision of 0.91, recall of 0.90, F1-score of 0.91, mAP@50 of 0.93, as outlined in Table 4.3.

Table 4.3 Accuracy Metrics of Traffic Signs

Class	Precision	Recall	F1 score	mAP@50
all	0.91	0.90	0.91	0.93
regulatory	0.90	0.86	0.88	0.88
speed	0.88	0.90	0.89	0.93
warning	0.95	0.92	0.94	0.97
guide	0.92	0.93	0.92	0.97

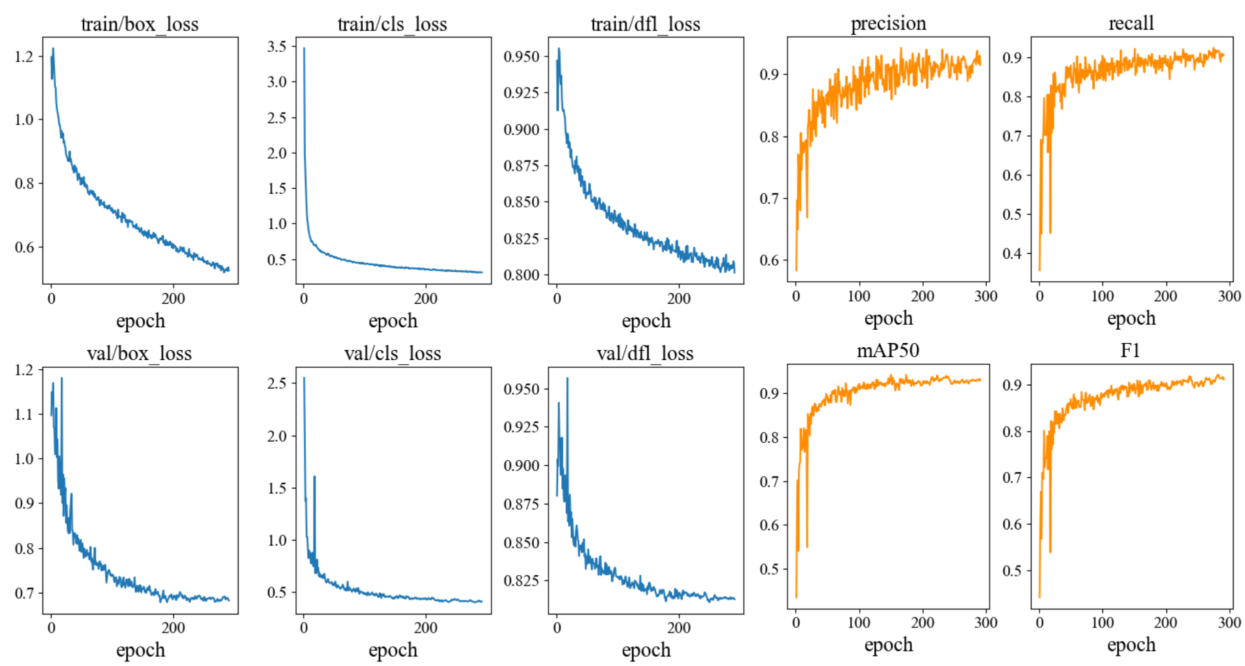

(a) Training Loss (b) Accuracy Metrics

Figure 4.7 Training Loss and Accuracy Metrics of Model for Traffic Signs

In Figure 4.8, a collection of detection results about traffic signs is showcased. The visual representations highlight the capabilities of the model in detecting various types of traffic signs, including guide signs (e.g., traffic movement directives), warning markers and signs, speed limit indicators, and regulatory signs. However, some roadside advertisement boards and panels with colors similar to traffic signs are mistakenly detected as traffic signs, as shown in Figure 4.9.

(a) Traffic Movement Guide Sign-1

(b) Traffic Movement Guide Sign-2

(c) Exit Guide and Warning Marker

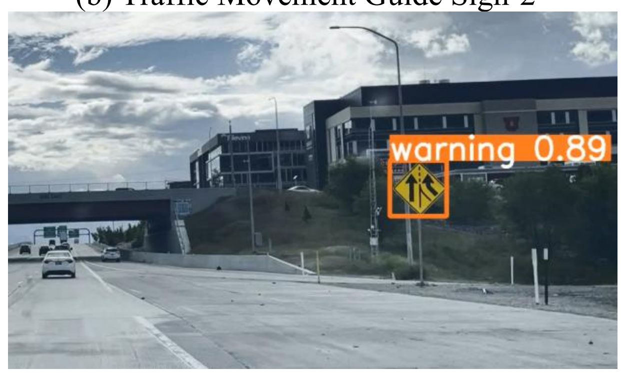

(d) Warning Sign

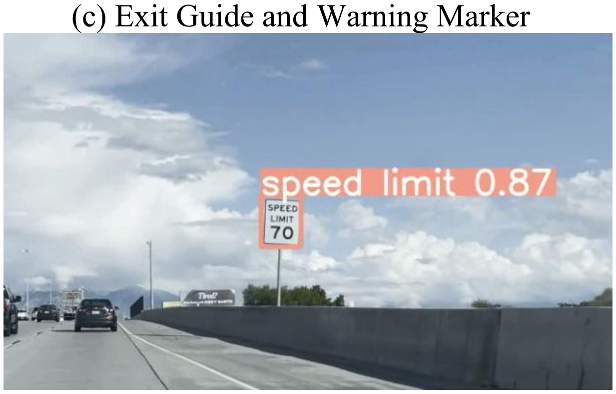

(e) Speed Limit Sign-1

(f) Speed Limit Sign-2

(g) Stop Sign and Street Guide (h) Do Not Enter and Street Guide

Figure 4.8 Examples of Detection Results of Traffic Signs

(a) Advertisement Board (b) Materials with Color Similar Traffic Signs

Figure 4.9 Examples of Wrong Detection of Traffic Signs

4.1.4 Identifying Guardrails and Barriers

There are 4,500 images labeled for guardrails and barriers, which are divided into 3,600 and 900 for training and validation, respectively. Figure 4.10 illustrates the accuracy metrics and training loss during the algorithm training process, and finally, the AI model reaches convergence. The best model training result was achieved at the epoch 250. The model precision is around 96% with a recall rate of 96%, F1 score of 96%, and mAP@50 0.97 (Table 4.4).

Table 4.4 Accuracy Metrics of Guardrails & Barriers

Class	Precision	Recall	F1 score	mAP@50
all	0.96	0.96	0.96	0.97
concrete	0.97	0.96	0.96	0.97
steel beam	0.95	0.97	0.96	0.97

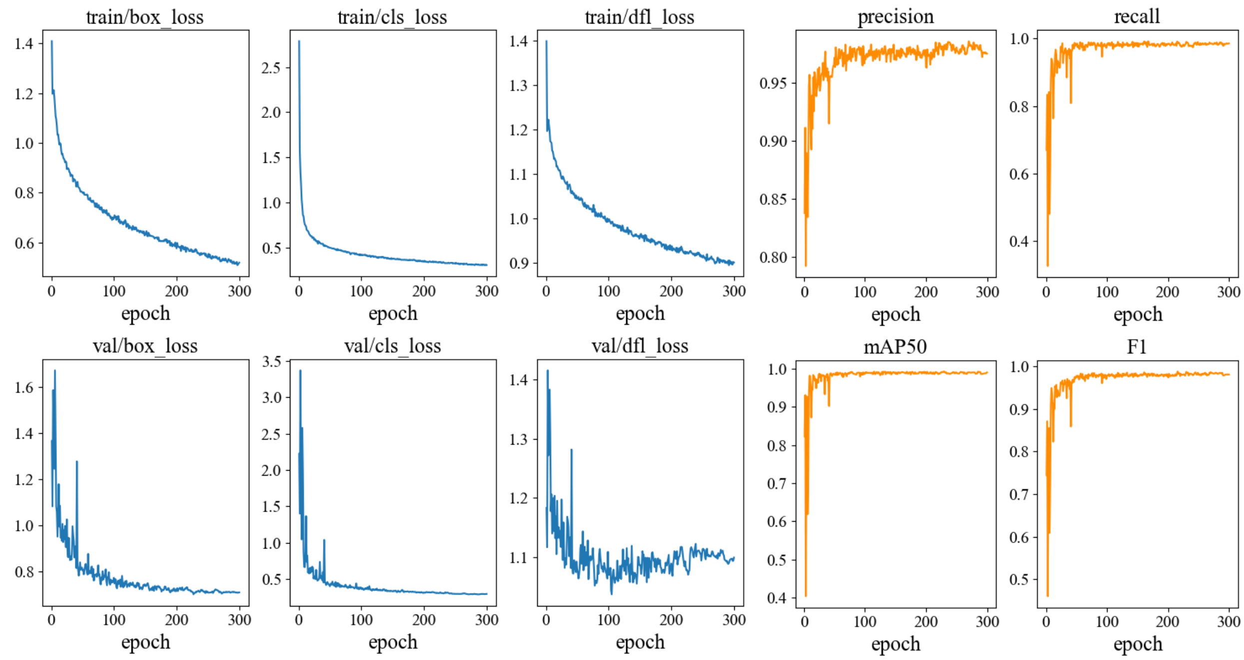

(a) Training Loss (b) Accuracy Metrics

Figure 4.10 Training loss and accuracy metrics of model training for guardrails

In Figure 4.11, a series of examples are shown presenting the successful detection of w-beam steel guardrails and concrete barriers by the developed model. Although the model demonstrates high accuracy in identifying steel guardrails and concrete barriers, it has some limitations. Notably, guardrails or barriers located far from the camera are often undetected, as illustrated in Figure 4.12.

(a) W-Beam Steel Guardrail

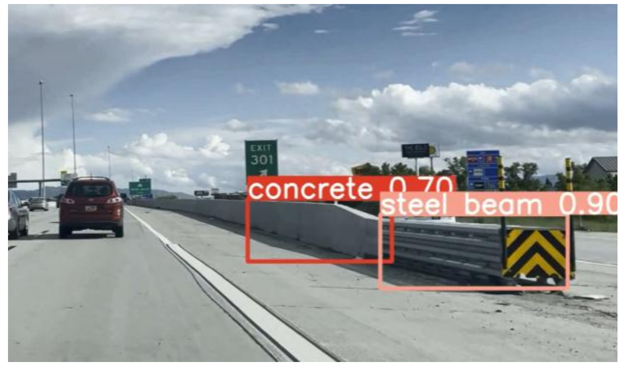

(b) Concrete Barrier and Steel Guardrail

(c) Concrete Barrier-1

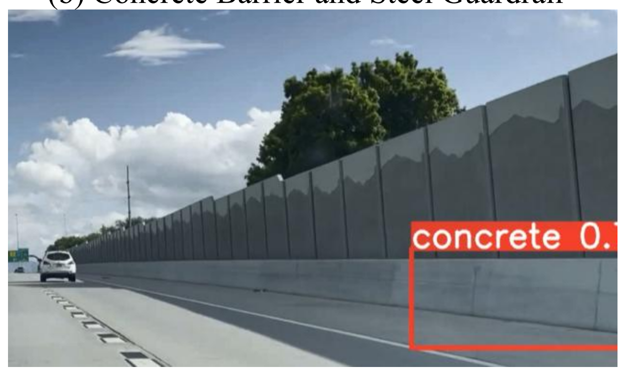

(d) Concrete Barrier-2

Figure 4.11 Examples of Detections Results of Guardrails and Barriers

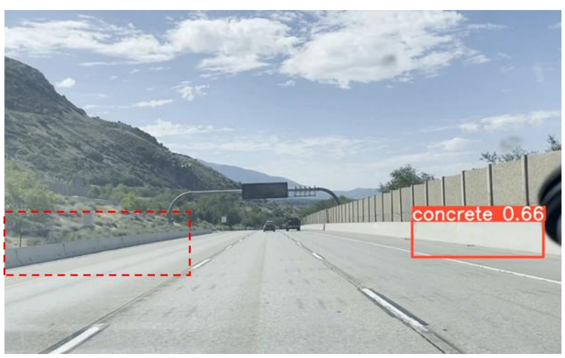

(a) Not Identifying Concrete Barrier-1

(b) Not Identifying Concrete Barrier-2

Figure 4.12 Examples of Wrong Detections of Guardrails and Barriers

4.2 Results of Object Counting

Based on the developed counting algorithm, we performed case studies on a 35-minute video shot along a highway section from Salt Lake City to Lehi, covering approximately 35 miles

(56.4 kilometers), as illustrated by the red route in Figure 4.13. The video captures objects of interest in this project, including pavement marking, traffic signs, litter, and guardrails.

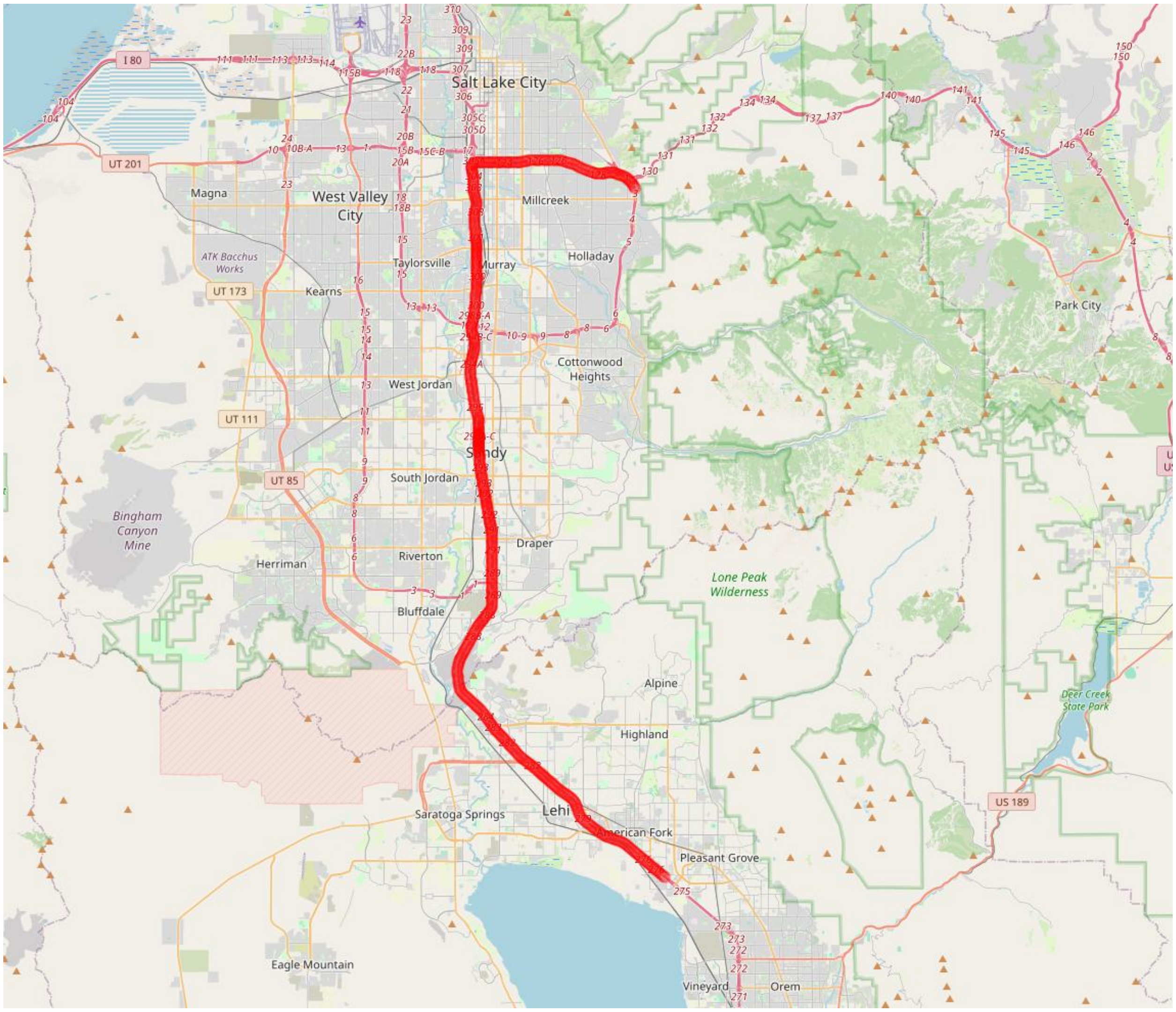

Figure 4.13 Case Study Area

The count results are updated and displayed in the top left corner of each frame, as depicted in Figure 4.14. The findings reveal that along the test route, there are 518 white faded markings, 33 instances of white litter, 263 instances of black litter, and 102 instances of dirt. Moreover, the models identify 136 warning signs, 296 guide signs, 181 speed limit signs, and 3 regulatory signs. Additionally, 41 w-beam steel guardrails and 669 concrete barriers are successfully detected.

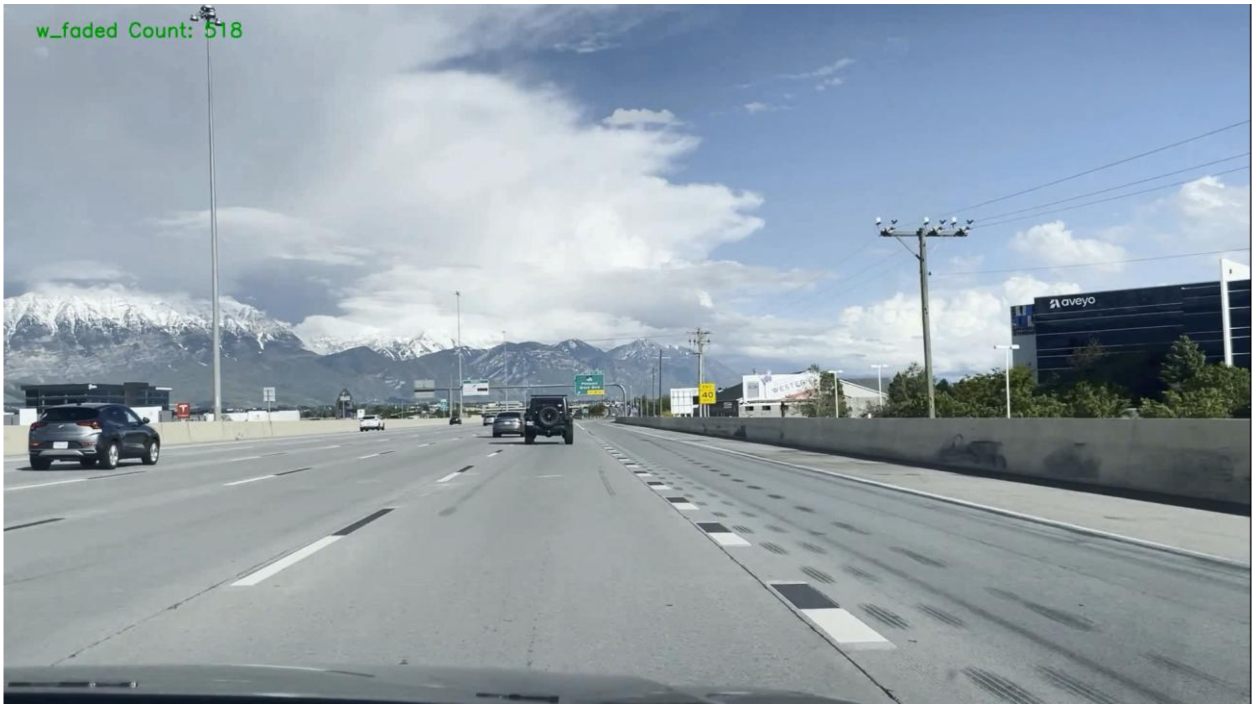

(a) Counting Results of Pavement Marking Issues

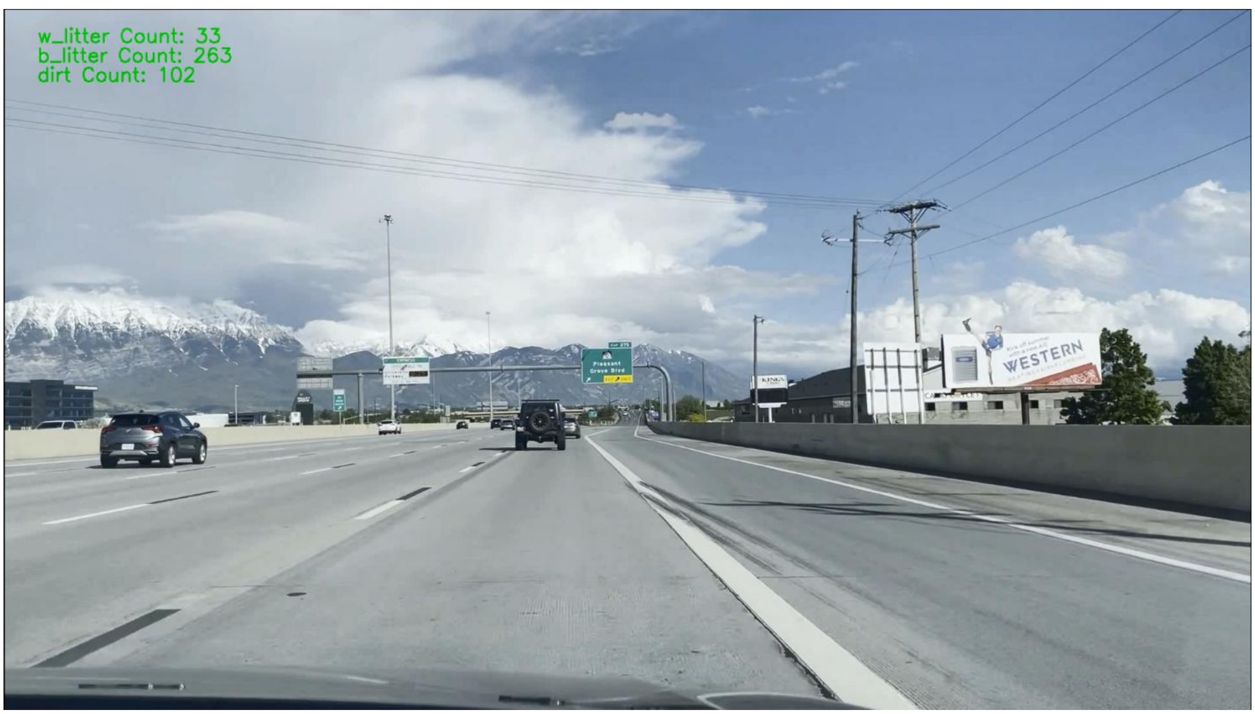

(b) Counting Results of Litter & Trash

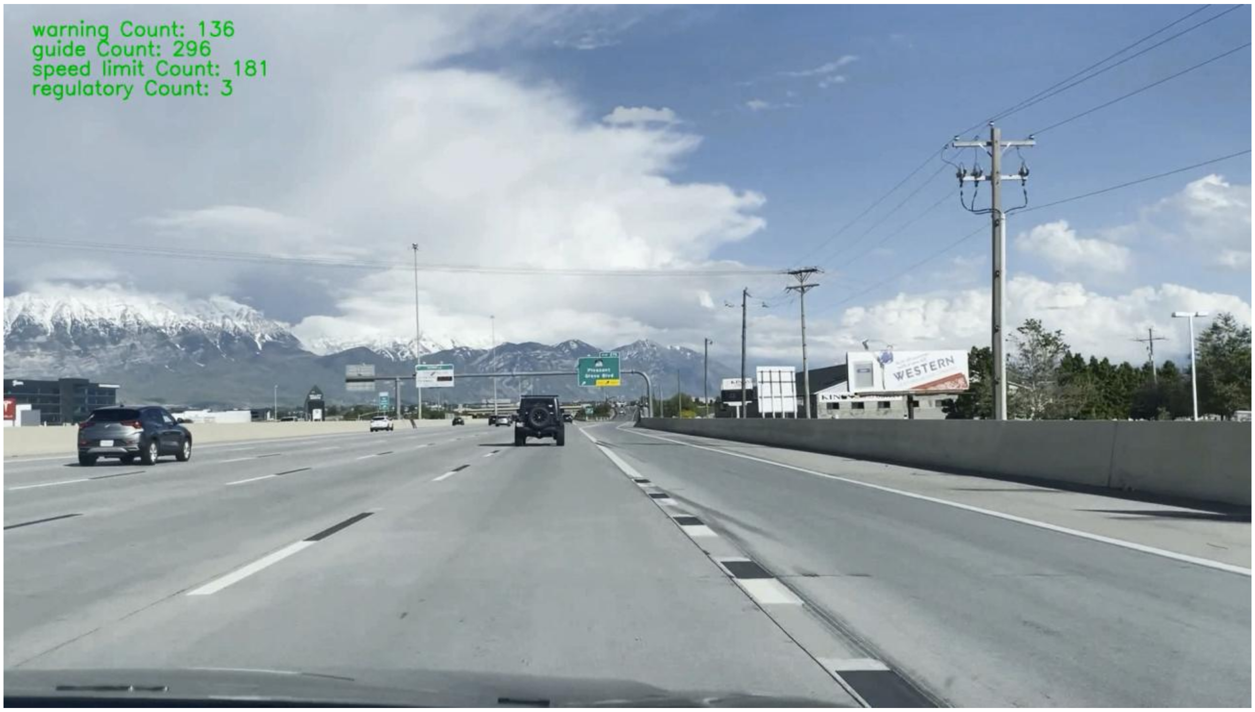

(c) Counting Results of Traffic Signs

(d) Counting Results of Guardrails &Barriers

Figure 4.14 Results of Object Counting

4.3 Results of Object Geolocation

4.3.1 Accuracy of Geolocation Model

A geolocation model has been developed to accurately locate identified objects with the assistance of a GPX tracker. Given the challenges associated with obtaining precise ground truth data for the exact locations of these objects, the performance of the model is validated through cross-section validations. To validate the model, out of 3500 continuous location records covering approximately 39 kilometers on a freeway (I-15), 175 record points (5% of the total records) were randomly selected as validation points, as depicted in Figure 4.15(a). The remaining points were used to predict the locations of the validation points, which were then compared against the true locations obtained from the GPX tracker.

The accuracy of the model is assessed by measuring the error, defined as the distance between the predicted location and the true location recorded by the GPX tracker. The error distributions for each point are visualized in Figure 4.15(b). The distance error ranges from less than 0.01 to 8.16 meters, with an average error of 0.27 meters (about 0.9 feet). Consequently, the developed geolocation model demonstrates decent performance in accurately estimating the locations of pavement marking issues.

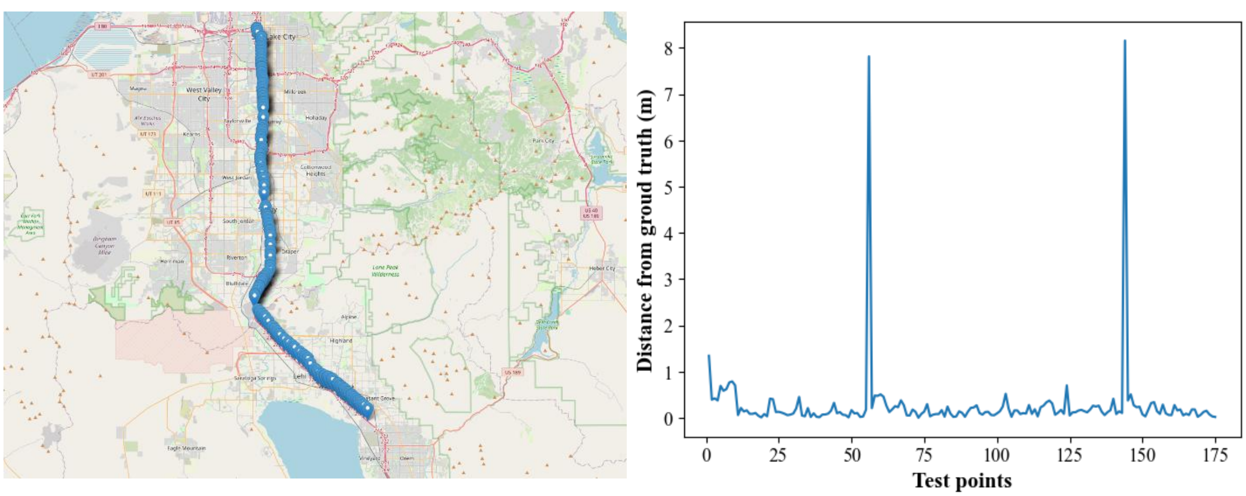

(a) Validation Points of Geolocation Model (b) Locating Error of Geolocation Model

Figure 4.15 Validation Points and Locating Error

4.3.2 Visualizing the Geolocation of Identified Objects

For visualizing the information of the identified objects, such as geolocation, object class, and inspection time, an interface has been developed using the Python package Folium. This interface is tailored to exhibit these details clearly and consisely. An example of this interface display can be viewed in Figure 4.16.

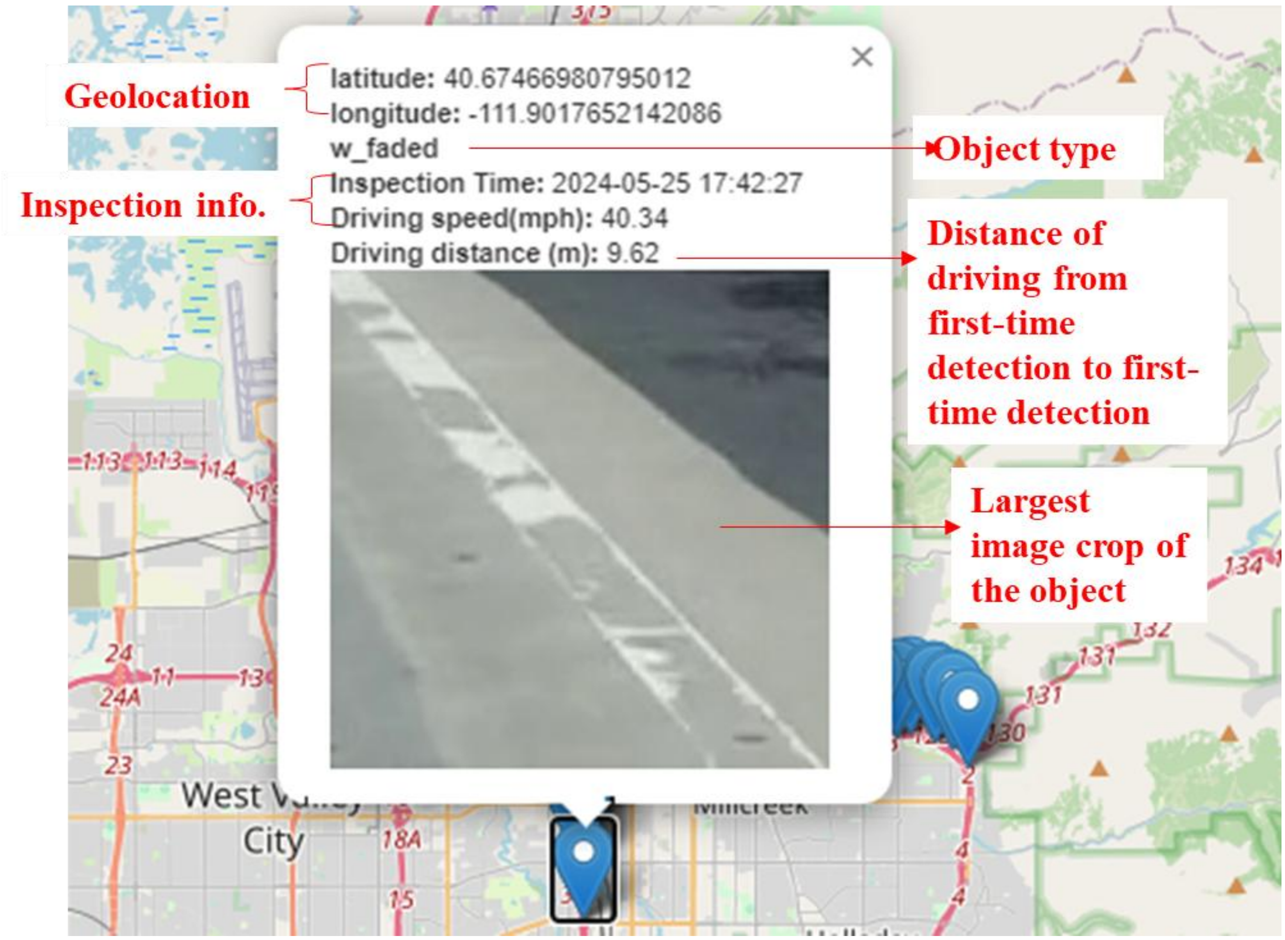

Figure 4.16 Example of Visualization

Specifically, the map generated using Folium features a pop-up window dedicated to each identified object. Within the pop-up window, the geolocation of the object is showcased, displaying the latitude and longitude coordinates, followed by the object type. Subsequently, the inspection time and the estimated driving speed inferred from the geolocation model are also delineated. Furthermore, a detailed view of the object is provided through the largest cropped image available. Moreover, for certain continuous objects within this project, i.e., faded markings and guardrails/barriers, we include additional information regarding the driving distance between the initial and final detections. While this driving distance may not reflect the actual size of the object, it serves as a comparative reference for assessing the sizes of different objects effectively.

4.3.3 Case Studies of Object Geolocation and Visualization

The geolocations of pavement marking issues along the test route are visually represented in Figure 4.17-(a), pinpointing each identified marking issue based on the inferred locations. Additionally, Figure 4.17 (b)-(c) are illustrative examples showcasing the visualization of white faded marking issues for further clarity and understanding.

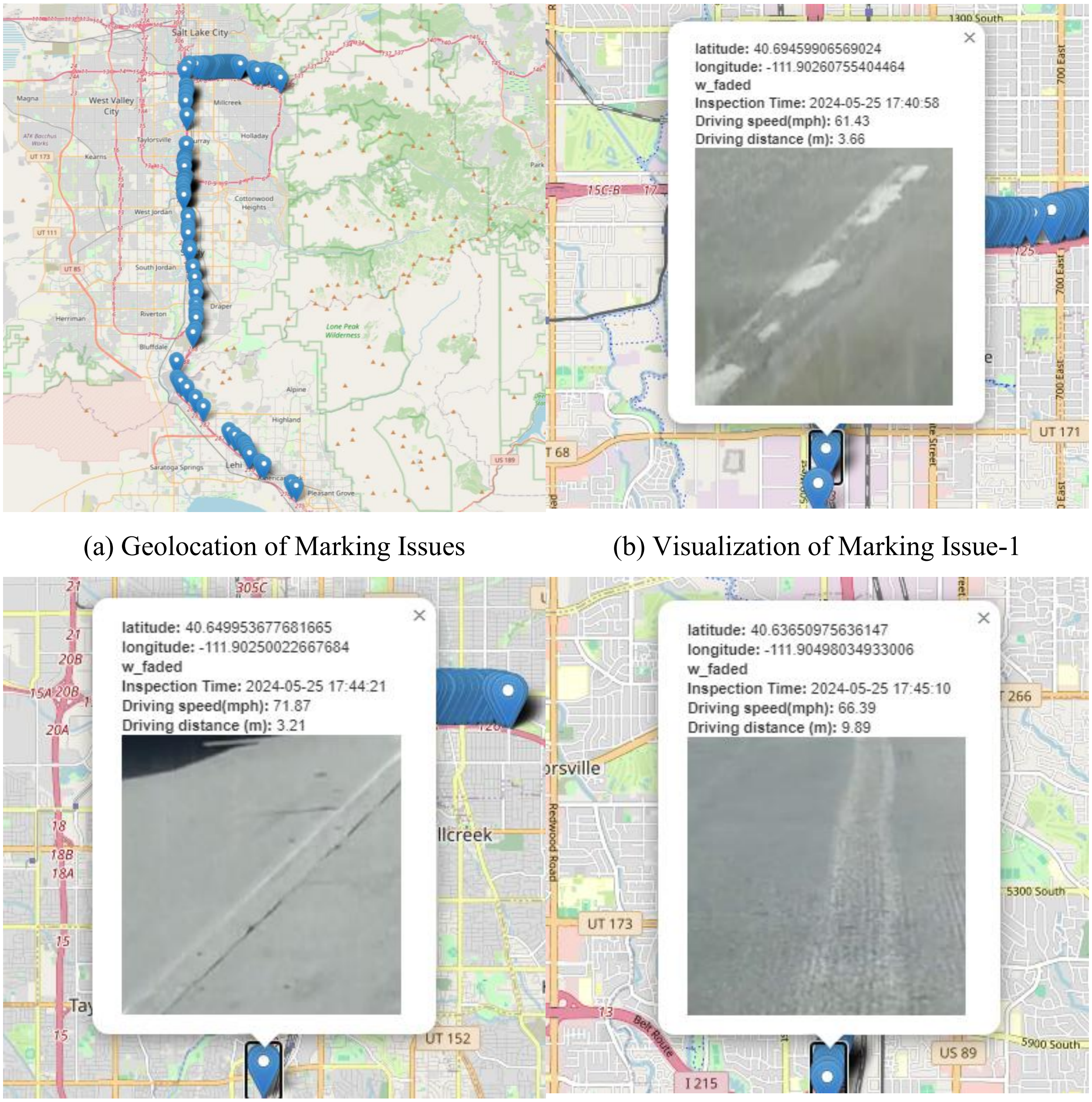

(a) Geolocation of Marking Issues (b) Visualization of Marking Issue-1

(c) Visualization of Marking Issue-2 (d) Visualization of Marking Issue-3

Figure 4.17 Geolocation and Visualization of Pavement Marking Issues

Figure 4.18-(a) showcases the geolocations of identified litter and trash along the test route, providing a detailed spatial overview of these findings. Furthermore, Figure 4.18 (b)-(d) offer

examples that visually present the details of various types of litter and trash, such as the location, litter type, inspection time, and a cropped image for enhanced visual reference.

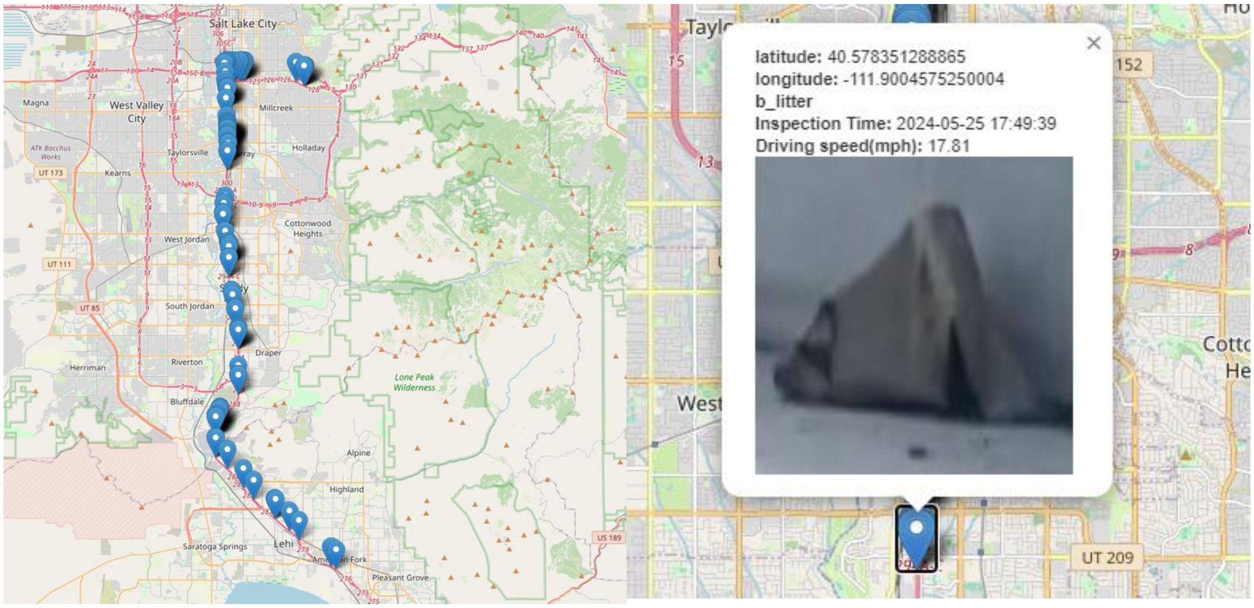

(a) Geolocation of Litter & Trash (b) Visualization of Black Litter

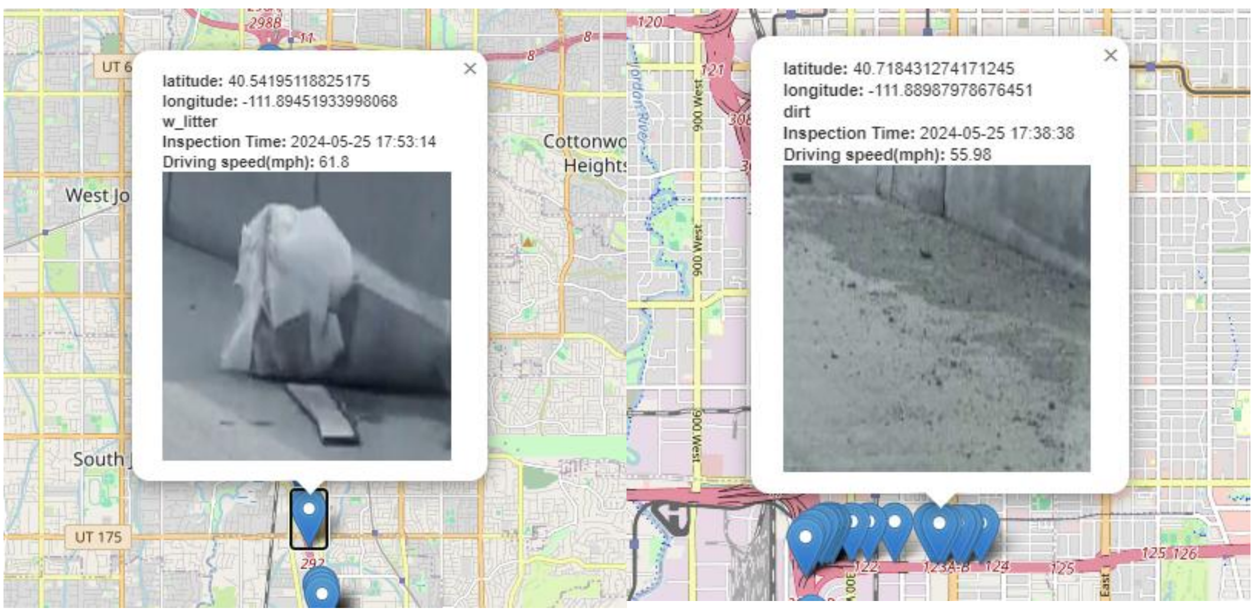

(c) Visualization of White Litter (b) Visualization of Dirt

Figure 4.18 Geolocation and Visualization of Litter & Trash

Figure 4.19-(a) showcases the locations of identified traffic signs on the test highway route. Additionally, Figure 4.19 (b)-(d) provide examples showing various traffic signs and their corresponding inspection details, including geolocations, types of traffic signs, inspection times, and cropped images for a comprehensive understanding of the traffic signs and conditions.

(a) Geolocation of Traffic Signs

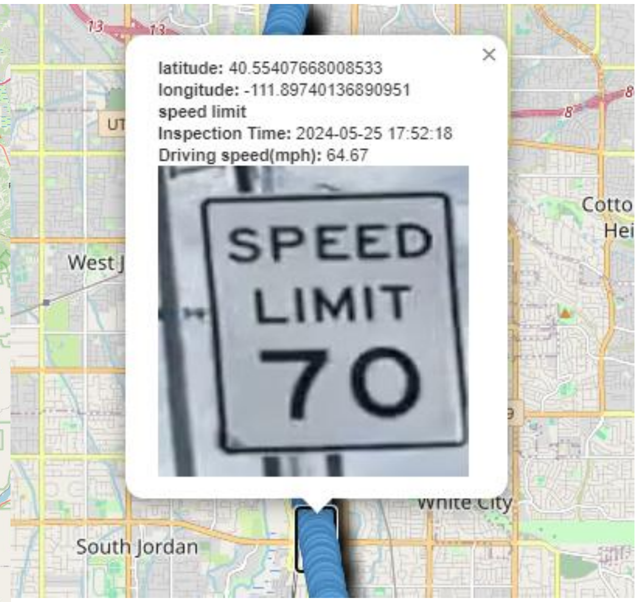

(b) Visualization of Speed Sign

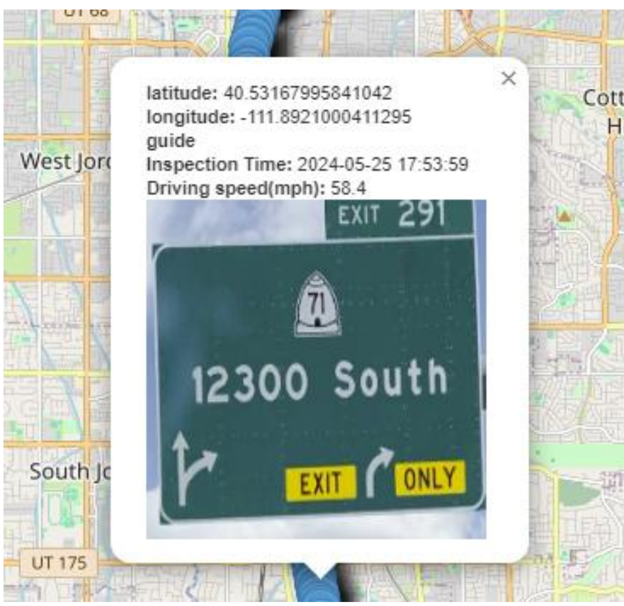

(c) Visualization of Warning Sign

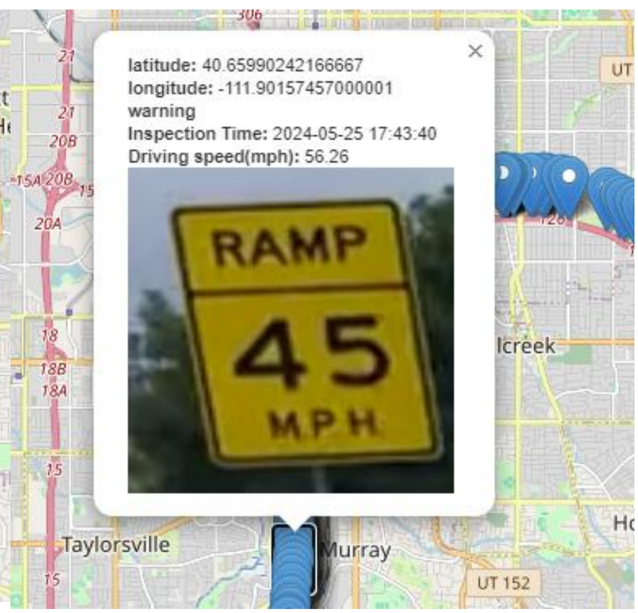

(d) Visualization of Warning Sign

Figure 4.19 Geolocation of Traffic Signs

Figure 4.20-(a) showcases the locations of the identified guardrails and barriers, offering a spatial representation of these transportation assets along the test route. Figure 4.20-(b) to Figure 4.20-(d) present examples that visually illustrate the identified and precisely pinpointed concrete barriers and W-beam steel guardrails.

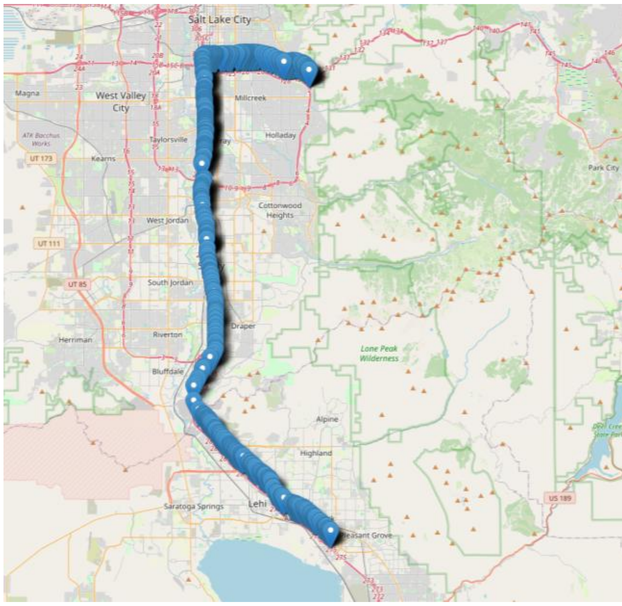

(a) Geolocation of Guardrails & Barriers

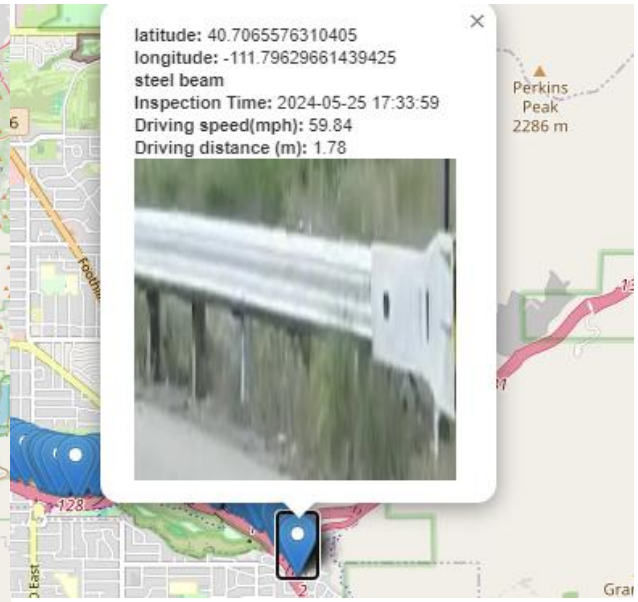

(b) Visualization of W-Beam Steel Guardrail

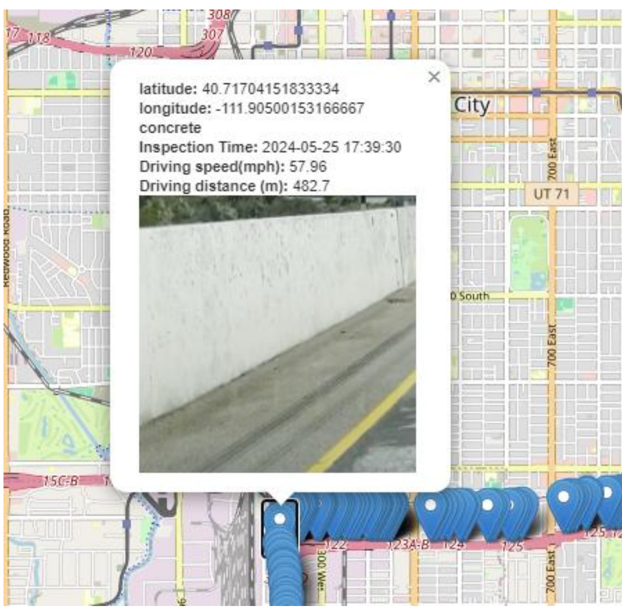

(c) Visualization of Concrete Barrier-1

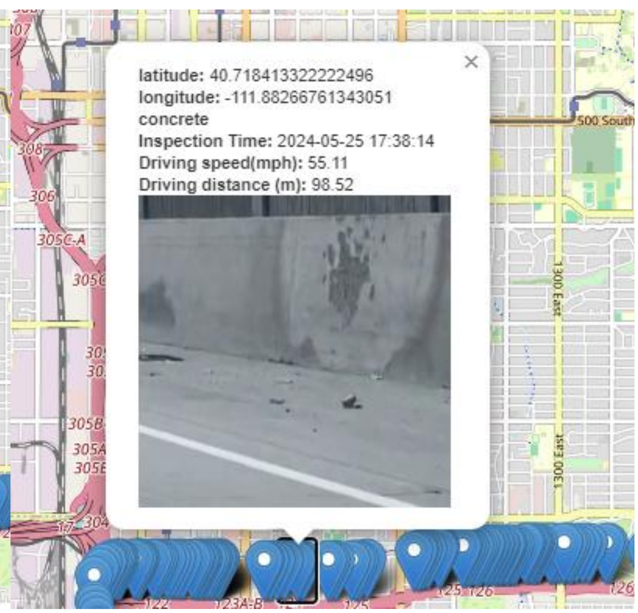

(d) Visualization of Concrete Barrier -2

Figure 4.20 Geolocation of Guardrails & Barriers

5.0 CONCLUSIONS

5.1 Summary of Findings

The project extends the AI packages developed in our prior UDOT Project (Contract No. 22-8099, Report No. UT-22.24) by expanding the dataset to around 5,000 images for each research task, encompassing pavement marking issues, litter & trash, traffic signs, and guardrails & barriers. These models are subsequently validated on a larger scale. Additionally, improvements have been made to the AI packages to enable object counting within a road section or video clip, geolocate identified objects using a phone-based GPS tracker, and visualize object details in a developed interface, including geolocations, object class, inspection time, and cropped images of the objects.

Specifically, we increased the training datasets for each project task, as follows:

(1) Pavement Marking Issues: 7,000 images were used to train the AI model for detecting pavement marking issues. These issues were classified into two classes by color: faded yellow markings ("y_faded") and faded white markings ("w_faded"). The AI model achieved a precision of 0.88, recall of 0.89, F1 score of 0.88, and mAP@50 of 0.93.

(2) Trash and Litter Identification: A dataset of 6,250 images was utilized to develop the AI model for trash and litter identification. The model categorized litter into four major classes: leaves, dirt, white litter ("w_litter"), and black litter ("b_litter"). The model attained a precision of 0.86, recall of 0.82, F1 score of 0.84, and mAP@50 of 0.88.

(3) Traffic Sign Identification: With 5,100 images, the AI model was trained for traffic sign identification. Traffic signs were classified into four categories: "regulatory," "speed," "warning," and "guide." The model exhibited accuracy metrics of 0.91 for precision, 0.90 for recall, 0.91 for the F1 score, and 0.93 for mAP@50.

(4) Guardrail and Barrier Identification: The AI model utilized 4,500 images for training to identify steel guardrails ("steel beam") and concrete barriers ("concrete"). The model demonstrated high accuracy with 0.96 precision, 0.96 recall, 0.96 F1 score, and 0.97 mAP@50.

Also, building upon object tracking, a specialized counting model was developed to quantify the identified objects within video clips or road sections. This model has been effectively employed to count the number of identified objects, specifically focusing on the objects of interest within this project. Notably, this model has been applied successfully on a test highway route in Utah, showcasing its practical application and reliability in real-world scenarios.

Moreover, expanding the capabilities further, a model was developed to estimate the locations of identified objects using time-based interpolations with the assistance of a mobile-phone-based GPS tracker (GPX tracker). This geolocation model, integrated with the detection model, demonstrates remarkable accuracy, with an average distance error of just 0.27 meters (about 0.9 feet), as validated through cross-section analysis. This precision underscores the reliability and effectiveness of the geolocation model in pinpointing the positions of identified objects with high fidelity, as demonstrated in a case study of a test highway route in Utah.

Finally, utilizing Folium (a Python package), an interactive interface was developed to visually represent the detailed information of these identified objects on a map. The display information consists of geolocation coordinates (i.e., latitude and longitude), object class, inspection time, and cropped images. The developed interface serves as a valuable tool for transportation authorities to comprehensively understand and assess the conditions of transportation assets through intuitive visualizations.

This project expands upon our previous work to enhance the detection of transportation assets, improving capabilities in identifying targeted transportation assets, while introducing additional functionalities, such as counting, geolocating, and visualizing these detected objects. These advancements facilitate more frequent inspections of transportation assets, contributing to the continual enhancement of road user safety.

5.2 Limitations

While significant progress has been achieved, certain limitations persist in our current system. In our counting model, due to the limitations of object tracking in video, objects detected only once are not included in our final count results. Moreover, the interface pop-up window of the visualization interface can only represent details for a single object. In cases where two or more detected objects have the largest crops in the same frame, only one object will be shown on the interactive map. Furthermore, the driving distance measured in the visualization model denotes the span between initial and final detections of the object (i.e., pavement marking issues and guardrails & barriers), which is not the actual object size. Future work could consider the offset distance for the video recording continuous objects, e.g., pavement markings or guardrails/barriers, to study and measure the actual size of each identified object more accurately.

6.0 RECOMMENDATIONS AND IMPLEMENTATION

6.1 Implementation Plan

The delivered models consist of four trained detectors tailored to different transportation assets: pavement marking issues, litter & trash, traffic signs, and guardrails & barriers. Also, the package includes a model for object counting, a model for geolocation and visualization, and brief documentation for running the provided codes (Model Note.docx in the shared folder). All AI models are developed in Python. To execute these models, a specific computational environment needs to be set up for YOLOv8 architecture. For practical implementation of the AI package, the following key steps should be followed:

1. Data Collection:

- Equip a mobile device with a GPS tracking application (e.g., GPX Tracker).
- Attach the mobile device to the windshield of a vehicle and record videos while simultaneously logging GPS data.
- Ensure the videos capture the targeted objects clearly by adjusting the camera angle, the position of the mobile device, and the driving lane as needed to maximize the visibility of the assets of interest.

2. Data Analysis:

- Export the recorded videos along with their associated GPS logs.
- Select the appropriate trained detector and run the object counting model. This step detects and counts the targeted objects, saving relevant detection data, including cropped images and associated data frames. The total number of identified objects will be displayed in the top-left corner of the video frames.
- Sequentially run the geolocation model to determine the precise locations of each identified object and visualize the results interactively on a map.

By following these steps, users can deploy the AI package efficiently to detect, count, geolocate, and visualize targeted objects within the collected video data. This process provides a powerful tool for enhancing transportation asset management and infrastructure evaluation.

6.2 Recommendations

This project developed a recommended AI package capable of automatically identifying, counting, and geolocating pavement marking issues, litter & trash, traffic signs, and guardrails & barriers. The solution provides a highly efficient, scalable, and cost-effective approach to transportation asset management, which enables UDOT to perform inspections on a frequent and large-scale basis. By leveraging AI, this package significantly reduces manual effort, enhances accuracy, and offers actionable insights for maintaining transportation asset quality.

Future efforts could further enhance the robustness and generalization of the AI models by increasing the size and diversity of the training datasets. Expanding the dataset to include additional scenarios, such as adverse weather conditions, low illumination, and varying levels of occlusion, will ensure reliable performance across a broader range of real-world conditions.

Additionally, future work could develop a user-friendly interface to facilitate the practical implementation of the AI package. Integrating the models into an intuitive user interface would simplify their deployment, allowing users to apply the AI package efficiently without requiring extensive technical expertise. Such advancements would ensure broader accessibility and usability, maximizing the impact of the package on transportation asset management.

REFERENCES

Akofio-Sowah, M.-A., Boadi, R., Amekudzi, A., & Meyer, M. (2014). Managing Ancillary Transportation Assets: The State of the Practice. *Journal of Infrastructure Systems*, *20*(1), 04013010. https://doi.org/10.1061/(ASCE)IS.1943-555X.0000162

Alzraiee, H., Leal Ruiz, A., & Sprotte, R. (2021). Detecting of Pavement Marking Defects Using Faster R-CNN. *Journal of Performance of Constructed Facilities*, *35*(4), 04021035. https://doi.org/10.1061/(ASCE)CF.1943-5509.0001606

Arezoumand, S., & Smadi, O. (2024). Equity in Transportation Asset Management: A Proposed Framework. *Algorithms*, *17*(7), Article 7. https://doi.org/10.3390/a17070305

ASTM. (2020). *Standard Practice for Evaluating Degree of Pavement Marking Line Wear* (Nos. D913-20; pp. 1–2). https://compass.astm.org/document/?contentcode=ASTM%7CD0913-20%7Cen-US

Balali, V., & Golparvar-Fard, M. (2014). *Video-Based Detection and Classification of US Traffic Signs and Mile Markers using Color Candidate Extraction and Feature-Based Recognition*. 858–866. https://doi.org/10.1061/9780784413616.107

Bronuela-Ambrocio, L. B., & Antes, E. R. D. (2023). Assessment of Longitudinal Pavement Marking Conditions Based on Deep Learning. *Philippine Engineering Jorunal*, *44*(1), 65–88.

Campbell, A., Both, A., & Sun, Q. (Chayn). (2019). Detecting and mapping traffic signs from Google Street View images using deep learning and GIS. *Computers, Environment and Urban Systems*, *77*, 101350. https://doi.org/10.1016/j.compenvurbsys.2019.101350

Cano-Ortiz, S., Pascual-Muñoz, P., & Castro-Fresno, D. (2022). Machine learning algorithms for monitoring pavement performance. *Automation in Construction*, *139*, 104309. https://doi.org/10.1016/j.autcon.2022.104309

Chang, C. M., & Vavrova, M. (2016). *Vulnerable User Road Safety Enhancements for Transportation Asset Management*. 238–246. https://doi.org/10.1061/9780784479926.022

Chehri, H., Chehri, A., & Saadane, R. (2021). Traffic Signs Detection and Recognition System in Snowy Environment Using Deep Learning. In M. Ben Ahmed, İ. Rakıp Karaș, D. Santos, O. Sergeyeva, & A. A. Boudhir (Eds.), *Innovations in Smart Cities Applications Volume 4* (pp. 503–513). Springer International Publishing. https://doi.org/10.1007/978-3-030-66840-2_38

Dowd, Z., Franz, A. Y., & Wasek, J. S. (2020). A Decision-Making Framework for Maintenance and Modernization of Transportation Infrastructure. *IEEE Transactions on Engineering Management*, *67*(1), 42–53. IEEE Transactions on Engineering Management. https://doi.org/10.1109/TEM.2018.2870326

Du, Y., Pan, N., Xu, Z., Deng, F., Shen, Y., & Kang, H. (2020). Pavement distress detection and classification based on YOLO network. *International Journal of Pavement Engineering*, 1–14. https://doi.org/10.1080/10298436.2020.1714047

Farhadmanesh, M., Cross, C., Mashhadi, A. H., Rashidi, A., & Wempen, J. (2021). Highway Asset and Pavement Condition Management using Mobile Photogrammetry. *Transportation Research Record*, *2675*(9), 296–307. https://doi.org/10.1177/03611981211001855

Fernández-Sanjurjo, M., Bosquet, B., Mucientes, M., & Brea, V. M. (2019). Realtime visual detection and tracking system for traffic monitoring. *Engineering Applications of Artificial Intelligence*, *85*, 410–420. https://doi.org/10.1016/j.engappai.2019.07.005

FHWA. (2009). *Manual on Uniform Traffic Control Devices (MUTCD) 2009 Edition*. https://mutcd.fhwa.dot.gov/pdfs/2009/pdf_index.htm

Ghosh, R., & Smadi, O. (2021). Automated Detection and Classification of Pavement Distresses using 3D Pavement Surface Images and Deep Learning. *Transportation Research Record*, 03611981211007481. https://doi.org/10.1177/03611981211007481

Gopalakrishnan, K., Khaitan, S. K., Choudhary, A., & Agrawal, A. (2017). Deep Convolutional Neural Networks with transfer learning for computer vision-based data-driven pavement distress detection. *Construction and Building Materials*, *157*, 322–330. https://doi.org/10.1016/j.conbuildmat.2017.09.110

Hoang, V.-D., Le, M.-H., Tran, T. T., & Pham, V.-H. (2018). Improving Traffic Signs Recognition Based Region Proposal and Deep Neural Networks. In N. T. Nguyen, D. H. Hoang, T.-P. Hong, H. Pham, & B. Trawiński (Eds.), *Intelligent Information and Database Systems* (pp. 604–613). Springer International Publishing. https://doi.org/10.1007/978-3-319-75420-8_57

Hou, Q., & Ai, C. (2022). An Automated Sound Barrier Inventory Method Using Mobile LiDAR. *Journal of Transportation Engineering, Part A: Systems*, *148*(10), 04022078. https://doi.org/10.1061/JTEPBS.0000732

Hou, Q., Ai, C., & Boudreau, N. (2022). Network-Level Guardrail Extraction Based on 3D Local

Features from Mobile LiDAR Sensor. *Journal of Computing in Civil Engineering*, *36*(6), 04022035. https://doi.org/10.1061/(ASCE)CP.1943-5487.0001049

Iparraguirre, O., Iturbe-Olleta, N., Brazalez, A., & Borro, D. (2022). Road Marking Damage Detection Based on Deep Learning for Infrastructure Evaluation in Emerging Autonomous Driving. *IEEE Transactions on Intelligent Transportation Systems*, *23*(11), 22378–22385. https://doi.org/10.1109/TITS.2022.3192916

Jin, H., Lan, Z., & He, X. (2021). On Highway Guardrail Detection Algorithm Based on Mask RCNN in Complex Environments. *2021 7th International Conference on Systems and Informatics (ICSAI)*, 1–6. https://doi.org/10.1109/ICSAI53574.2021.9664044

Kang, K., Chen, D., Peng, C., Koo, D., Kang, T., & Kim, J. (2020). Development of an Automated Visibility Analysis Framework for Pavement Markings Based on the Deep Learning Approach. *Remote Sensing*, *12*(22), Article 22. https://doi.org/10.3390/rs12223837

Karballaeezadeh, N., Zaremotekhases, F., Shamshirband, S., Mosavi, A., Nabipour, N., Csiba, P., & Várkonyi-Kóczy, A. R. (2020). Intelligent Road Inspection with Advanced Machine Learning; Hybrid Prediction Models for Smart Mobility and Transportation Maintenance Systems. *Energies*, *13*(7), Article 7. https://doi.org/10.3390/en13071718

Kargah-Ostadi, N., Waqar, A., & Hanif, A. (2020). Automated Realtime Roadway Asset Inventory using Artificial Intelligence. *Transportation Research Record*, *2674*(11), 220–234. https://doi.org/10.1177/0361198120944926

Karsten, L., Gargoum, S., Saleh, M., & El-Basyouny, K. (2021). Automated Framework to Audit Traffic Signs Using Remote Sensing Data. *Journal of Infrastructure Systems*, *27*(3), (ASCE)IS.1943-555X.0000618, 04021014. https://doi.org/10.1061/(ASCE)IS.1943-555X.0000618

Kawano, M., Mikami, K., Yokoyama, S., Yonezawa, T., & Nakazawa, J. (2017). Road marking blur detection with drive recorder. *2017 IEEE International Conference on Big Data (Big Data)*, 4092–4097. https://doi.org/10.1109/BigData.2017.8258427

Khan, J. A., Yeo, D., & Shin, H. (2018). New Dark Area Sensitive Tone Mapping for Deep Learning Based Traffic Sign Recognition. *Sensors*, *18*(11), Article 11. https://doi.org/10.3390/s18113776

Kim, S., Kim, S., Uh, Y., & Byun, H. (2012). Color and shape feature-based detection of speed sign in realtime. *2012 IEEE International Conference on Systems, Man, and Cybernetics*

(SMC), 663–666. https://ieeexplore.ieee.org/abstract/document/6377802/

Koch, C., Jog, G. M., & Brilakis, I. (2013). Automated Pothole Distress Assessment Using Asphalt Pavement Video Data. *Journal of Computing in Civil Engineering*, *27*(4), 370–378. https://doi.org/10.1061/(ASCE)CP.1943-5487.0000232

Kong, W., Zhong, T., Mai, X., Zhang, S., Chen, M., & Lv, G. (2022). Automatic Detection and Assessment of Pavement Marking Defects with Street View Imagery at the City Scale. *Remote Sensing*, *14*(16), Article 16. https://doi.org/10.3390/rs14164037

Kuang, B., Chen, J., & Yang, X. T. (2022). *Mobile Phone-Based Artificial Intelligence Development for Maintenance Asset Management* (No. UT-22.24). https://rosap.ntl.bts.gov/view/dot/66158

Kuhn, B. T., Jasek, D., Carson, J., Theiss, L., Songchitruksa, P., Perkins, J., Yang, Y., & Mwakalong, J. (2011). *Research on Asset Management for Safety and Operations*. Citeseer. https://citeseerx.ist.psu.edu/document?repid=rep1&type=pdf&doi=2ede668aaae606cedb9ced3b50035369c54d3842

Le, N. D., Tran, D., Harper, C. M., & Sturgill, R. E. (2024). Exploring Inspection Technologies for Highway Infrastructure During Construction and Asset Management. *Transportation Research Record*, 03611981241260690. https://doi.org/10.1177/03611981241260690

Lee, S., & Cho, B. H. (2023). Evaluating Pavement Lane Markings in Metropolitan Road Networks with a Vehicle-Mounted Retroreflectometer and AI-Based Image Processing Techniques. *Remote Sensing*, *15*(7), Article 7. https://doi.org/10.3390/rs15071812

Liu, Y., Ge, Z., Lv, G., & Wang, S. (2018). Research on Automatic Garbage Detection System Based on Deep Learning and Narrowband Internet of Things. *Journal of Physics: Conference Series*, *1069*, 012032. https://doi.org/10.1088/1742-6596/1069/1/012032

Liu, Z., Li, Z., Li, L., & Yang, H. (2020). Complex background classification network: A deep learning method for urban images classification. *Computers & Electrical Engineering*, *87*, 106771. https://doi.org/10.1016/j.compeleceng.2020.106771

Ma, D., Fang, H., Wang, N., Zhang, C., Dong, J., & Hu, H. (2022). Automatic Detection and Counting System for Pavement Cracks Based on PCGAN and YOLO-MF. *IEEE Transactions on Intelligent Transportation Systems*, *23*(11), 22166–22178. IEEE Transactions on Intelligent Transportation Systems.

https://doi.org/10.1109/TITS.2022.3161960

Maeda, H., Sekimoto, Y., Seto, T., Kashiyama, T., & Omata, H. (2018). Road Damage Detection and Classification Using Deep Neural Networks with Smartphone Images. *Computer-Aided Civil and Infrastructure Engineering*, *33*(12), 1127–1141. https://doi.org/10.1111/mice.12387

Majidifard, H., Jin, P., Adu-Gyamfi, Y., & Buttlar, W. G. (2020). Pavement Image Datasets: A New Benchmark Dataset to Classify and Densify Pavement Distresses. *Transportation Research Record*, *2674*(2), 328–339. https://doi.org/10.1177/0361198120907283

Mandal, V., Mussah, A. R., & Adu-Gyamfi, Y. (2020). Deep Learning Frameworks for Pavement Distress Classification: A Comparative Analysis. *2020 IEEE International Conference on Big Data (Big Data)*, 5577–5583. https://doi.org/10.1109/BigData50022.2020.9378047

Mandhati, S. R., Deshapriya, N. L., Mendis, C. L., Gunasekara, K., Yrle, F., Chaksan, A., & Sanjeev, S. (2024). *pLitterStreet: Street Level Plastic Litter Detection and Mapping* (No. arXiv:2401.14719). arXiv. https://doi.org/10.48550/arXiv.2401.14719

Nguyen, S. D., Tran, V. P., Tran, T. S., Lee, H. J., & Flores, J. M. (2023). Automated Segmentation and Deterioration Determination of Road Markings. *Journal of Transportation Engineering, Part B: Pavements*, *149*(3), 04023013. https://doi.org/10.1061/JPEODX.PVENG-1181

Okpe, J. B., & Idachaba, F. E. (2023). *Development of an Iot Model for Pothole Detection , Counting and Geolocation* (SSRN Scholarly Paper No. 4671532). https://doi.org/10.2139/ssrn.4671532

Peng, J., Wang, W., Hu, W., Ai, C., Xu, X., Shi, Y., Wang, J., Ran, Z., & Qiu, S. (2024). Automated detection and quantification of pavement cracking around manhole. *Engineering Applications of Artificial Intelligence*, *130*, 107778. https://doi.org/10.1016/j.engappai.2023.107778

Pike, A. M., Kuchangi, S. P., & Benz, R. J. (2010). Quantitative versus Qualitative Assessment of Pavement Marking Visibility. *Transportation Research Record*, *2169*(1), 88–94. https://doi.org/10.3141/2169-10

Rad, M. S., Von Kaenel, A., Droux, A., Tieche, F., Ouerhani, N., Ekenel, H. K., & Thiran, J.-P. (2017). A Computer Vision System to Localize and Classify Wastes on the Streets. In M. Liu, H. Chen, & M. Vincze (Eds.), *Computer Vision Systems* (Vol. 10528, pp. 195–204).

Springer International Publishing. https://doi.org/10.1007/978-3-319-68345-4_18

Radopoulou, S. C., & Brilakis, I. (2015). Patch detection for pavement assessment. *Automation in Construction*, *53*, 95–104. https://doi.org/10.1016/j.autcon.2015.03.010

Redmon, J., Divvala, S., Girshick, R., & Farhadi, A. (2016). You Only Look Once: Unified, Realtime Object Detection. *2016 IEEE Conference on Computer Vision and Pattern Recognition (CVPR)*, 779–788. https://doi.org/10.1109/CVPR.2016.91

Sayyad, S., Parmar, S., Jadhav, M., & Khadayate, K. (2020). Realtime Garbage, Potholes and Manholes Monitoring System using Deep Learning Techniques. *2020 4th International Conference on Trends in Electronics and Informatics (ICOEI)(48184)*, 826–831. https://doi.org/10.1109/ICOEI48184.2020.9143030

Sinha, K. C., Labi, S., & Agbelie, B. R. D. K. (2017). Transportation infrastructure asset management in the new millennium: Continuing issues, and emerging challenges and opportunities. *Transportmetrica A: Transport Science*, *13*(7), 591–606. https://doi.org/10.1080/23249935.2017.1308977

Souza, V. M. A., Giusti, R., & Batista, A. J. L. (2018). Asfault: A low-cost system to evaluate pavement conditions in realtime using smartphones and machine learning. *Pervasive and Mobile Computing*, *51*, 121–137. https://doi.org/10.1016/j.pmcj.2018.10.008

Sun, Y., Tang, H., & Zhang, H. (2024). Automatic Detection of Pavement Marking Defects in Road Inspection Images Using Deep Learning. *Journal of Performance of Constructed Facilities*, *38*(2), 04024002. https://doi.org/10.1061/JPCFEV.CFENG-4619

Tabernik, D., & Skočaj, D. (2020). Deep Learning for Large-Scale Traffic-Sign Detection and Recognition. *IEEE Transactions on Intelligent Transportation Systems*, *21*(4), 1427–1440. IEEE Transactions on Intelligent Transportation Systems. https://doi.org/10.1109/TITS.2019.2913588

Tepljakov, A., Riid, A., Pihlak, R., Vassiljeva, K., & Petlenkov, E. (2019). Deep Learning for Detection of Pavement Distress using Non-ideal Photographic Images. *2019 42nd International Conference on Telecommunications and Signal Processing (TSP)*, 195–200. https://doi.org/10.1109/TSP.2019.8769086

V, S., Tangade, S., K, P. P., J P, S., Azam, F., & L, A. G. (2022). Realtime Litter Recognition Using Improved YOLOv4 Tiny Algorithm. *2022 IEEE 2nd Mysore Sub Section International Conference (MysuruCon)*, 1–5.

https://doi.org/10.1109/MysuruCon55714.2022.9972356

Wang, K. C. P., Zhang, A., Li, J. Q., Fei, Y., Chen, C., & Li, B. (2017). *Deep Learning for Asphalt Pavement Cracking Recognition Using Convolutional Neural Network*. 166–177. https://doi.org/10.1061/9780784480922.015

Wang, N., Shang, L., & Song, X. (2023). A Transformer-Optimized Deep Learning Network for Road Damage Detection and Tracking. *Sensors*, *23*(17), Article 17. https://doi.org/10.3390/s23177395

Wei, C., Li, S., Wu, K., Zhang, Z., & Wang, Y. (2021). Damage inspection for road markings based on images with hierarchical semantic segmentation strategy and dynamic homography estimation. *Automation in Construction*, *131*, 103876. https://doi.org/10.1016/j.autcon.2021.103876

Wen, T., Ding, S., Lang, H., Lu, J. J., Yuan, Y., Peng, Y., Chen, J., & Wang, A. (2022). Automated pavement distress segmentation on asphalt surfaces using a deep learning network. *International Journal of Pavement Engineering*, *0*(0), 1–14. https://doi.org/10.1080/10298436.2022.2027414

Wickramasinghe, K. S., & Ganegoda, G. U. (2020). Pedestrian Detection, Tracking, Counting, Waiting Time Calculation and Trajectory Detection for Pedestrian Crossings Traffic light systems. *2020 20th International Conference on Advances in ICT for Emerging Regions (ICTer)*, 172–177. https://doi.org/10.1109/ICTer51097.2020.9325479

Wojke, N., Bewley, A., & Paulus, D. (2017). Simple online and realtime tracking with a deep association metric. *2017 IEEE International Conference on Image Processing (ICIP)*, 3645–3649. https://doi.org/10.1109/ICIP.2017.8296962

Wu, T.-W., Zhang, H., Peng, W., Lü, F., & He, P.-J. (2023). Applications of convolutional neural networks for intelligent waste identification and recycling: A review. *Resources, Conservation and Recycling*, *190*, 106813. https://doi.org/10.1016/j.resconrec.2022.106813

Xu, S., Wang, J., Wu, P., Shou, W., Wang, X., & Chen, M. (2021). Vision-Based Pavement Marking Detection and Condition Assessment—A Case Study. *Applied Sciences*, *11*(7), Article 7. https://doi.org/10.3390/app11073152

Zakeri, H., Nejad, F. M., & Fahimifar, A. (2017). Image Based Techniques for Crack Detection, Classification and Quantification in Asphalt Pavement: A Review. *Archives of*

Computational Methods in Engineering, *24*(4), 935–977. https://doi.org/10.1007/s11831-016-9194-z

Zhang, P., Zhao, Q., Gao, J., Li, W., & Lu, J. (2019). Urban Street Cleanliness Assessment Using Mobile Edge Computing and Deep Learning. *IEEE Access*, *7*, 63550–63563. IEEE Access. https://doi.org/10.1109/ACCESS.2019.2914270

Zhang, Y., & Ge, H. (2012). Assessment of Presence Conditions of Pavement Markings with Image Processing. *Transportation Research Record*, *2272*(1), 94–102. https://doi.org/10.3141/2272-11